DETERMINATION OF THERMAL AND ELECTRICAL CONDUCTIVITY, EMITTANCE AND THOMSON COEFFICIENT AT HIGH TEMPERATURES BY DIRECT HEATING METHODS

Raymond E. Taylor, et al

Purdue University
Lafayette, Indiana

October 1969

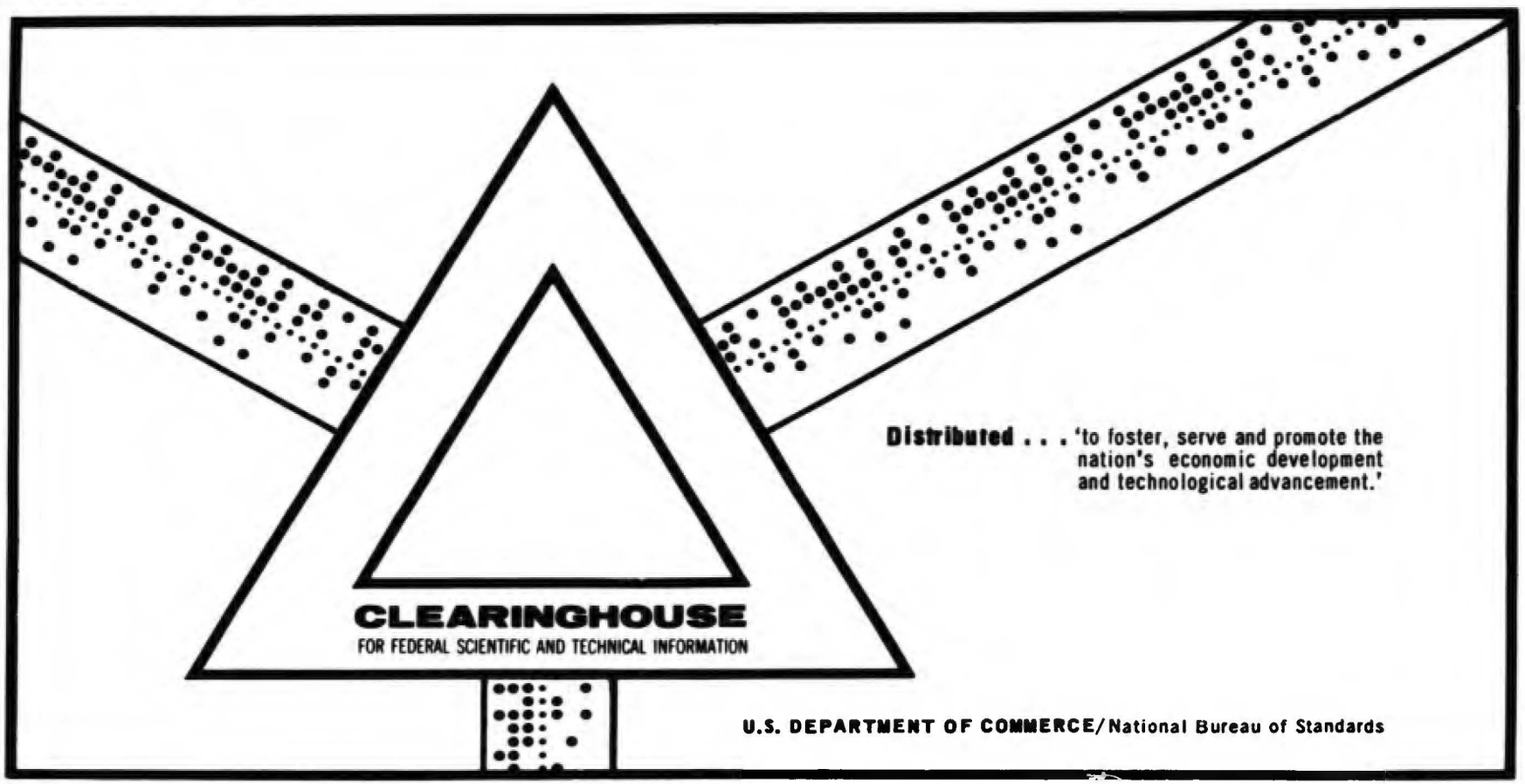

AFML-TR-69-277

DETERMINATION OF THERMAL AND ELECTRICAL CONDUCTIVITY, EMITTANCE AND THOMSON COEFFICIENT AT HIGH TEMPERATURES BY DIRECT HEATING METHODS

R. E. Taylor
F. E. Davis
R. W. Powell
W. D. Kimbrough

Thermophysical Properties Research Center
Purdue University

TECHNICAL REPORT AFML-TR-69-277
October 1969

Air Force Materials Laboratory
Air Force Systems Command
Wright-Patterson Air Force Base, Ohio

NOTICES

When Government drawings, specifications, or other data are used for any purpose other than in connection with a definitely related Government procurement operation, the United States Government thereby incurs no responsibility nor any obligation whatsoever; and the fact that the Government may have formulated, furnished, or in any way supplied the said drawings, specifications, or other data, is not to be regarded by implication or otherwise as in any manner licensing the holder or any other person or corporation, or conveying any rights or permission to manufacture, use, or sell any patented invention that may in any way be related thereto. This document has been approved for public release and sale; its distribution is unlimited.

Copies of this report should not be returned unless return is required by security considerations, contractual obligations, or notice on a specific document.

DETERMINATION OF THERMAL AND ELECTRICAL CONDUCTIVITY, EMITTANCE AND THOMSON COEFFICIENT AT HIGH TEMPERATURES BY DIRECT HEATING METHODS

R.E. Taylor
F.E. Davis
R.W. Powell
W.D. Kimbrough

FOREWORD

This report was prepared by the Thermophysical Properties Research Center, Purdue University, on Air Force Contract F33615-69-C-1229. The work was initiated under Project No. 7381, "Materials Applications", Task No. 738106, "Design Information Development". Dr.Merrill L. Minges of the Air Force Materials Laboratory, MAAS, monitored the contract which covered the period July 1, 1968 to June 30, 1969. This report was submitted July 15, 1969.

This technical report has been reviewed and is approved.

L. N. Hjelm, Chief
Materials Support Division
Air Force Materials Laboratory

ABSTRACT

Progress on a program for evaluating direct electrical heating methods for high temperature thermal conductivity determinations is presented. Recent modifications, which increased the temperature capabilities of the apparatus, protected the samples from contamination and improved the accuracy and simplicity of the measurements, are described.

A method for calculating the thermal conductivity using any three temperature versus position data points (3-point method) of a temperature profile was devised. This development permits conductivity determinations to be made from any portion of a temperature profile in contrast to the previously reported 2-point method which requires data from the central portion of the profile. Since small errors in the emittance cause large errors in the computed conductivity values derived from the central portion, the 3-point method represents a significant advance. Using this 3-point method, hundreds of conductivity values can be calculated per temperature profile. Computational schemes which utilize multiple data points or the output of the 3-point program are being developed. Substantial improvement in the accuracy and reproducibility of the computed thermal conductivity values have been obtained using these schemes. In addition, values for the Thomson coefficient are derived.

Data on thermal conductivity, total hemispherical emittance, spectral emittance (0.65 microns), electrical resistivity, and Thomson coefficient for tantalum, ATJS graphite and tungsten to about 2700 K are presented. Reproducibilities were generally about ±0.7% for the electrical resistivity, ±1% for the total hemispherical emittance, ±1% for the spectral emittance and ±3% for the thermal conductivity (multiple data point computations).

TABLE OF CONTENTS

LIST OF ILLUSTRATIONS

LIST OF TABLES

NOMENCLATURE

Symbol	Definition
A	Cross-sectional area perpendicular to Z-axis
BI	Brightness temperature
F	$I^2\rho/A^2 - P\epsilon_H\sigma(T^4 - T_0^4)/A$
I	Electric current
I_s	Electric current through short sample
I_∞	Electric current through infinitely long sample
$\vec{J}$	Current density ($\vec{I}/A$)
L	Length along Z-axis
P	Circumference of sample
T	Temperature of the sample at any location Z
TT	True temperature
T_c	Temperature at center of sample
T_0	Ambient temperature
T_∞	Temperature at center of infinitely long sample
V	Voltage drop
W	Watts
Z	Length coordinate along longitudinal axis of sample
Z(1),Z(2)	Positions along sample
ϵ_H	Total hemispherical emittance
$\epsilon_{0.65}$	Spectral emittance at 0.65 microns
β	Constant which is determined graphically
λ	Thermal conductivity
μ	Thomson coefficient
ρ	Electrical resistivity
σ	Stefan- Boltzmann constant

I. INTRODUCTION

There are only a few practical and reliable methods for measuring thermal conductivity at high temperatures. One of these methods, perhaps the simplest experimentally, is termed the direct electrical heating method. It involves heating long thin wires, rods or tubes by passing regulated current (I) through the specimens and measuring potential gradients and temperatures.

A general equation describing steady state energy transport through the sample under vacuum while being heated electrically is:

$$\lambda\frac{d^2T}{dZ^2} + \frac{I^2\rho}{A^2} - \frac{P\epsilon_H\sigma}{A}(T^4 - T_0^4) - \mu\frac{I}{A}\frac{dT}{dZ} = 0 \qquad \text{Eq. (1)}$$

where λ is the thermal conductivity, ρ is the electrical resistivity, ϵ_H is the total hemispherical emittance, μ is the Thomson coefficient, A is the cross-sectional area, P is the circumference, σ is the Stefan-Boltzmann constant, T is the sample temperature, and T_0 is the ambient temperature. Because Eq. (1) is a second-order non-linear differential equation which has no closed solution, various researchers have neglected certain terms or made restrictive mathematical approximations in order to obtain conductivity values from their experimental data. This has led to a multitude of techniques and variants of this general classification starting with the Kohlrausch technique, which was used before 1900.

Analyses of the data obtained by various researchers using these variants have revealed that the potential of the general method has not been fully realized, nor have the results obtained using the various techniques yielded consistent, reliable data. A previous report[1] from this laboratory outlines the more widely used techniques which fall under this general classification and derives the associated mathematical relations. A second report[2] describes the experimental arrangement to evaluate the techniques and gives preliminary results using stainless steel as the test material. That report also discusses data handling procedures which eliminate the need for the commonly used mathematical approximations and discusses some of the errors and limitations involved in the use of these approximations. The present report discusses recent modifications to the experimental apparatus and the advances in the data handling procedures. These procedures incorporate temperature-dependent properties and also yield values for the Thomson coefficient. The errors associated with specific techniques can be determined by comparing

thermal conductivity values computed using the appropriate mathematical approximations to those obtained from the numerical solution of the general equation, employing the same set of experimental data. The development of practical methods to obtain the numerical solution of the general equation has eliminated the need for using the variants and has, in effect, rendered the previous techniques obsolete.

II. EXPERIMENTAL APPARATUS AND PROCEDURES

A. Experimental Apparatus

The experimental apparatus has been described in previous reports[1, 2] and only a brief general description will be presented here. However, recent modifications will be discussed in some detail. These modifications were made primarily to raise the upper limit of the temperature capabilities of the apparatus, protect the sample from contamination, increase the accuracy and simplify the resistivity determination.

The sample, in the form of a wire or thin rod or tube, is supported vertically between two electrodes. The upper electrode is movable in that it can be positioned at any height, but after positioning it is rigidly clamped. The lower electrode is movable and permits relatively free sample expansion and contraction. The electrodes are designed so that the specimen can extend through them. Thus, the electrode separation distance is adjustable and any portion of a long (up to 14") sample may be positioned between the electrode clamps.

The sample holder (Figure 1) is contained within a large vacuum bell jar (Figure 2) which is raised and lowered by a power-driven hoist. Vacuum in the low 10^{-7} torr range is routinely achieved within a few hours and vacuum in the mid 10^{-8} torr range can be attained with longer pump-out times. The water-cooled bell jar features two vertical optical windows (visible in Figure 2) and an internal window shutter to protect one of the windows during the time intervals between pyrometer measurements. The bell jar rests on a feed-through collar which contains rotary feed-throughs, instrumentation leads, electrical connections and water lines. Instrumentation read-out is accomplished using a central, guarded six-dial potentiometric facility (not visible in Figure 2). Power to the sample and heaters is supplied by regulated DC power supplies. A 500 ampere, 50 volt supply*, transformer, calibrated shunt, reversing switches and remote control circuitry has been installed for sample operation at temperatures above 1800 K while the power supplies described

*Sorensen Model CRD40-500A

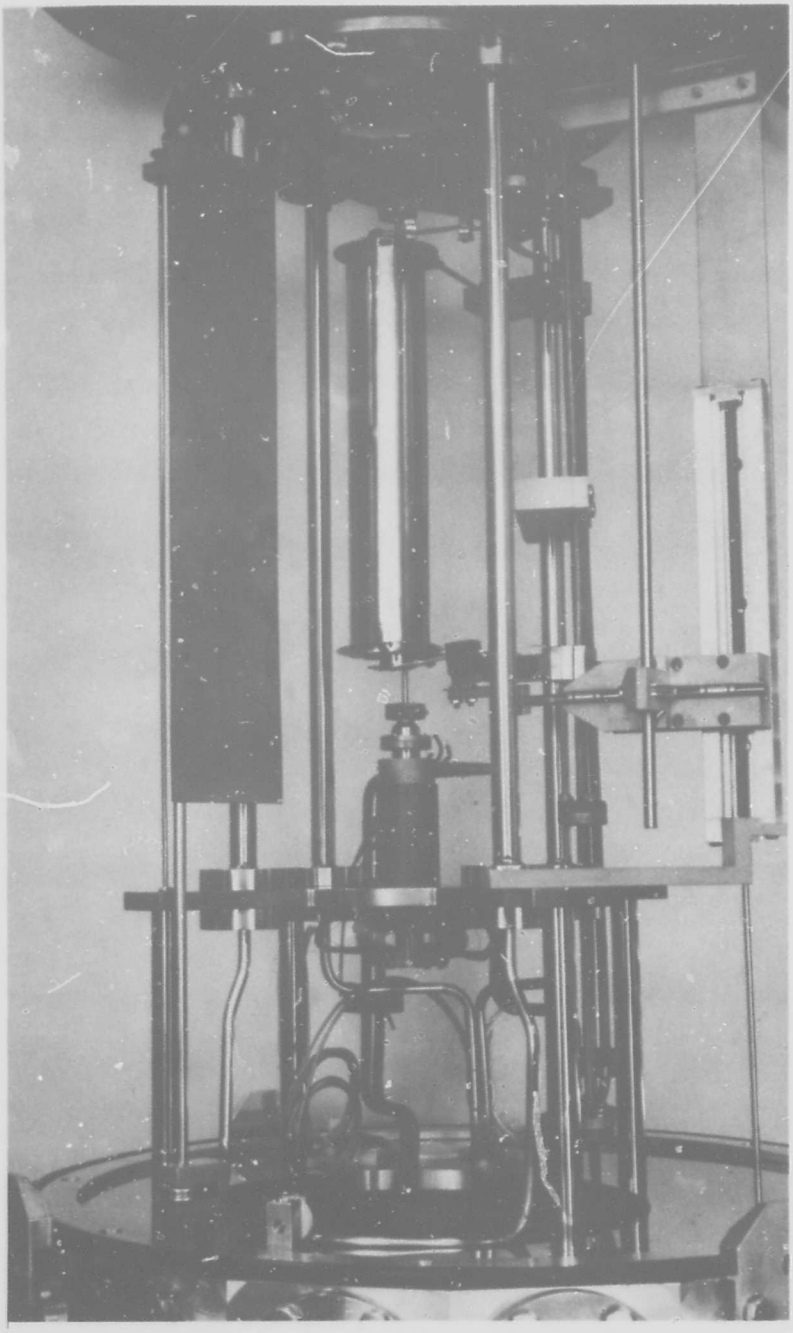

Figure 1

Close-Up of Sample Holder, Heater and Radiation Shields

Note: Reverse page 4 is blank.

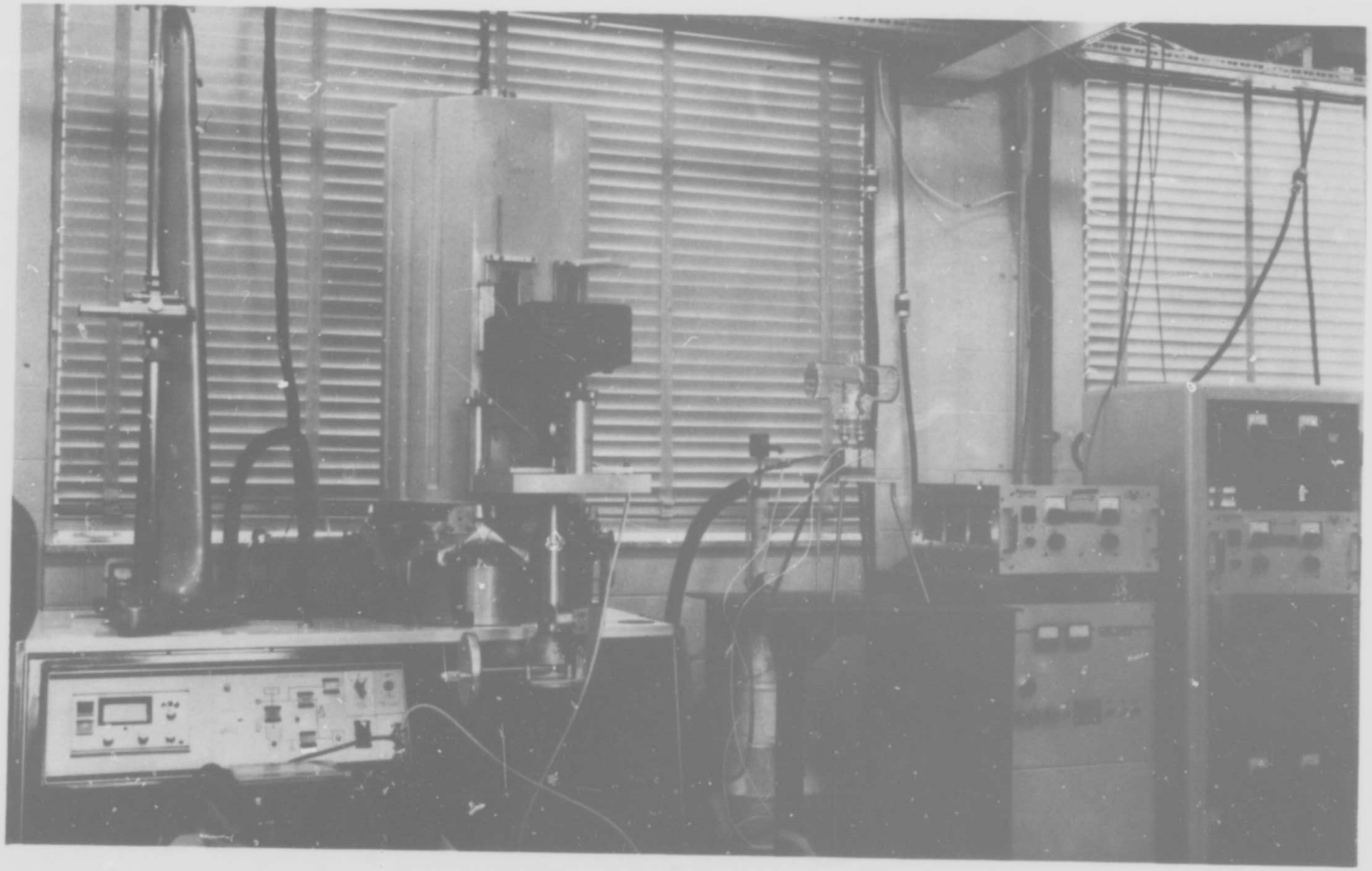

FIGURE 2 DIRECT HEATING APPARATUS

Note: Reverse page 6 is blank.

in previous reports[1,2] are used for lower sample temperatures, the heaters for the gettering system, and for electrical resistivity measurements when the sample is heated by a surrounding tube heater (Figure 1).

Modifications to the apparatus were made in an attempt to eliminate the contamination of metal samples which had been noted previously. Backstreaming of oil from the diffusion pump past the water baffle and liquid nitrogen cold trap was one possible source of contamination. Consequently, a new diffusion pump oil (Vacoil), which reportedly reduced backstreaming by a factor of ten, was used in place of Dow 704. As a further means of reducing backstreaming, an additional cold trap was designed, fabricated and installed just below the gate valve. This trap rests on the present liquid nitrogen trap and is cooled by conduction to this trap. The new trap, which consists of three six-inch copper disks with appropriate holes and spacers, reaches 100 K within one hour after the liquid nitrogen trap is filled. A gettering system, consisting of one mil tantalum sheet heated to a dull red, was installed near the base plate.

A second possible source of contamination was associated with the black coating used on the bell jar interior to reduce reflection. In the past, spots have been noted on this coating, indicating that seepage may be occurring through this coating; consequently, the coating was removed.

Since making these changes, no surface films have been observed on metal samples heated above 1500 K. However, emissivity changes are still noted on initial heating of metallic samples. Recrystallization appears to be a major cause, hence all metallic samples are pre-heated to induce recrystallization prior to thermal conductivity measurements.

An alternate optical path for monitoring sample temperatures has been provided when the quartz viewing window is shielded internally by the shutter. The quartz window now tends to remain much cleaner and no change in the optical transmission was noted when a tungsten sample was held at 2770 K for one hour. A monitoring device to determine window cleanliness during operation has been built and tested. This device employs a reflected beam from the front surface and therefore no parts are needed inside the vacuum enclosure.

Three automatic optical pyrometers are available for measuring brightness temperatures. These pyrometers are the Leeds and Northrup Model 8641 (shown in Figure 4 of reference 2), Leeds and Northrup Model 8640 (Figure 4) and the Pyrometer Instrument Co. Photomatic Model A-3 (Figure 2). During temperature profile meas-

urements, the pyrometer rests on a separate stand (Figure 2) equipped with rack and pinion for raising and lowering the pyrometer and with a turntable to facilitate focusing the pyrometer onto the sample surface. A blackbody lamp[3], purported to be reproducible to ± 0.1 C, is mounted on a movable platform (Figure 2) and has been used to check the Photomatic Pyrometer. Because of target size restrictions, the blackbody lamp cannot be used to check either Leeds and Northrup instrument. However, the calibration of all three pyrometers can be checked using a copper point blackbody[4] (shown in Figure 4).

One important modification to the experimental apparatus is the inclusion of a sample heater for resistivity measurements. This is included in Figure 1. The 2 mil tantalum tube heater and its associated shields which surround the sample are supported by water-cooled stainless steel columns. A movable clamp (Figure 1) is attached to the lower electrode of the heater so that the heater may be raised and lowered and/or rotated during operation. This feature permits the small hole in the heater to remain in alignment with a hole in a "clamp-on" blackbody used to measure sample temperatures.

The brightness of the surface of a 0.125" diameter sample enclosed by a tube heater and radiation shields and viewed through small holes in the heater and shields will be enhanced by reflection from the heater. Thus, a hole in the sample (very undesirable for the present application) or a clamp-on blackbody is required in order to measure the temperature accurately by optical pyrometry. A clamp-on blackbody and clamp-on voltage probes are shown to the right in Figure 3. This clamp-on blackbody is made of graphite and is held in place by a graphite set screw. It contains a 0.050" diameter hole 0.170" deep. It is interesting to note that, due to reflection from the heater, the effective spectral emittance of the blackbody hole may be greater or equal to 1.0 depending upon the length-to-diameter ratio of the hole and the material used. For example, using a tantalum clamp-on blackbody 0.320" OD with a 0.050" diameter by 0.090" deep hole, the effective spectral emittance was 1 04. Using the graphite clamp-on blackbody shown in Figure 3, the effective spectral emittance was 1.00. This value of spectral emittance was also obtained using a tantalum ring containing a graphite insert containing a hole comparable to the geometry of the hole shown in Figure 3.

Clamp-on voltage probes (Figure 3) consisting of three pointed tantalum set screws mounted in a tantalum ring and with tantalum wire for voltage leads are used for resistivity measurements when spot-welding voltage probes to the sample surface is not practical. Movable spring-loaded voltage probes are used during emittance

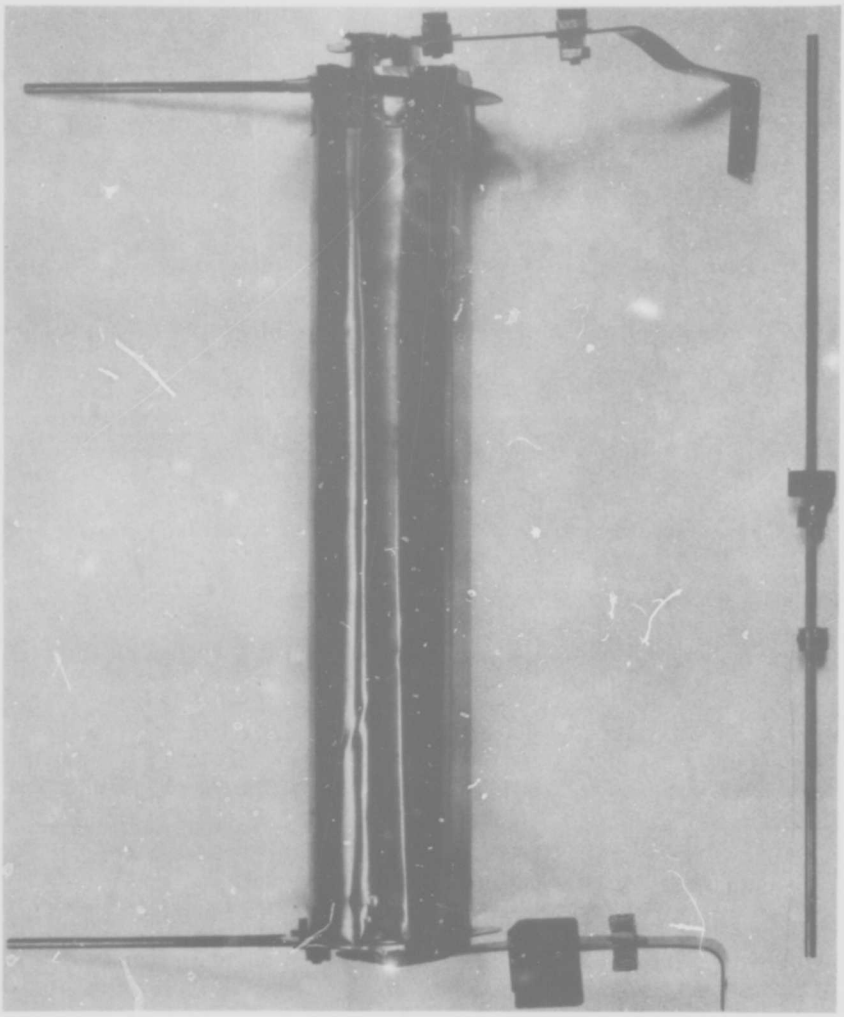

FIGURE 3 SAMPLE WITH CLAMP-ON BLACK BODY AND CLAMP-ON VOLTAGE PROBES

Note: Reverse page 10 is blank.

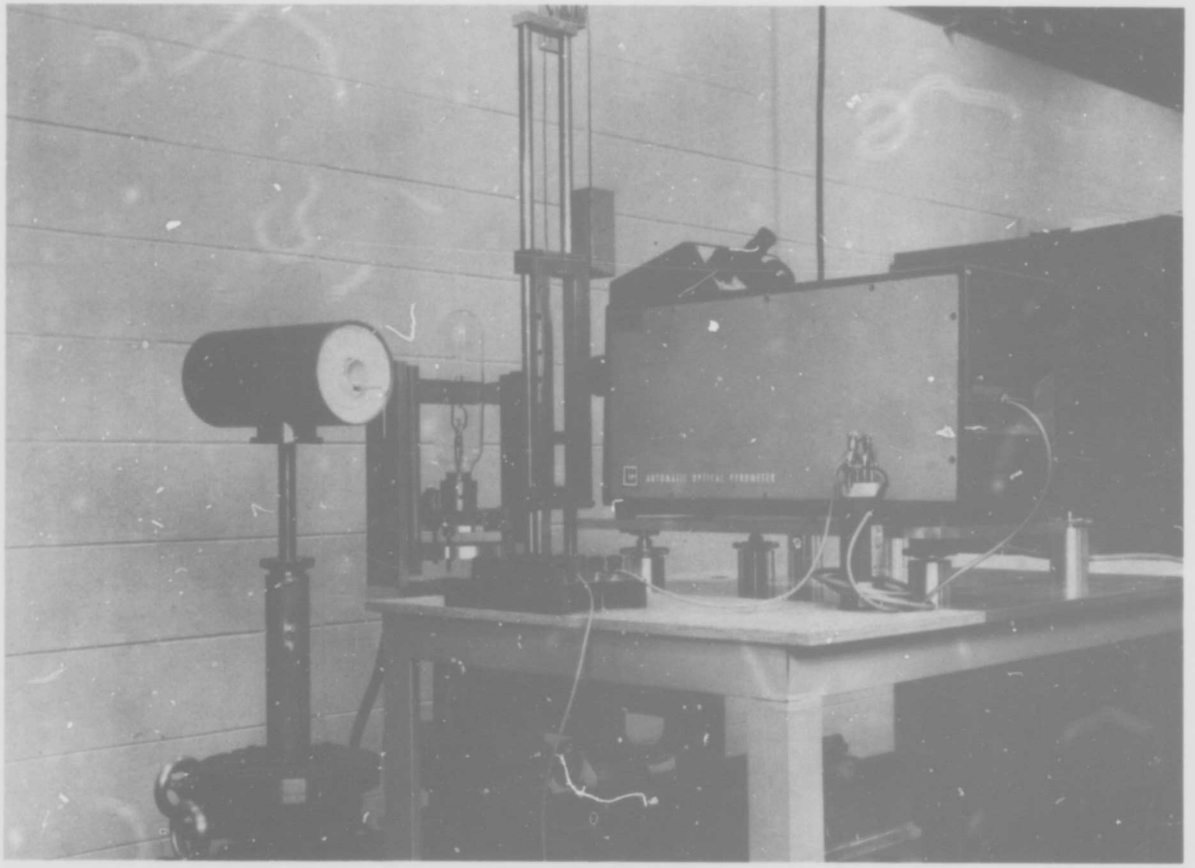

FIGURE 4 PYROMETER CALIBRATION FACILITY

Note: Reverse page 12 is blank.

determinations when spot-welded probes are not feasible. The mechanism employed to position the sample heater (Figure 1) is used with the spring-loaded probes.

B. Experimental Procedures

The experimental procedures for a determination of the thermophysical properties currently being measured are as follows:

(1) The cross-sectional area and density of the sample are determined.

(2) If voltage probe wires can be spot-welded to the sample, this is done and the distance between the voltage probes is accurately determined.

(3) The sample is mounted in the apparatus between the electrodes. If the sample is not long enough to insure that a central region will be at a uniform temperature during direct heating, extensions are connected onto the sample ends using couplings and set screws.

(4) The sample is pre-tested by heating under high vacuum to a temperature higher than that for which measurements are desired.

(5) The stability of the total hemispherical emittance is established by monitoring brightness temperatures and electrical resistivity during both steady state and temperature cycling.

(6) After a stable surface has been achieved, the electrical resistivity is measured as a function of brightness temperature. "Hemispherical emittances"(using brightness temperatures instead of true temperatures) are also calculated and checked for reproducibility.

(7) The sample length is effectively shortened by moving the electrode clamps closer together. Temperature profiles at several different maximum temperatures are measured. It is often necessary to use several different effective sample lengths in order to obtain optimum temperature profiles.

(8) The electrode clamps are returned to their original position for a long sample and resistivity and "hemispherical emittances" are redetermined as a function of brightness temperature. If the results do not agree with the previous results, steps 7 and 8 must be repeated until measurements made before and after temperature profile determinations are in agreement.

(9) Window corrections using the setup in Figure 4 are determined.

(10) Electrical resistivity as a function of true temperature is determined using a sample heater and radiation shields (Figure 1).

(11) Using these data, brightness temperatures (BT) are converted to true temperature (TT). Then $\epsilon_{0.65}$ (spectral emittance at 0.65 microns) and ϵ_H (total hemispherical emittance) as functions of TT are computed.

(12) Polynomial fits for resistivity, total hemispherical emittance and spectral emittance at 0.65 microns as functions of true temperature are determined. Temperature profiles Z(BT) are converted to Z(TT).

(13) Values for thermal conductivity and Thomson coefficients are computed using the procedures discussed in the following section.

C. Data Handling Procedures

Equation (1) involves four thermophysical properties ($\lambda, \rho, \epsilon_H$ and μ) in addition to first and second temperature derivatives. Let us assume that we know $\rho(T)$ and $\epsilon_H(T)$ and that the term containing μ is negligible compared to the other terms in Eq. (1). Then three conditions are required in order to obtain a value for λ because the conductivity is unknown and a second order differential equation is involved. Procedures for obtaining numerical solutions for λ start at some point on the curve or use some other information at this point (initial conditions) and attempt to go through some other point on the curve or fulfill some condition at that point (boundary conditions). Two initial conditions could be the maximum temperature and $dT/dZ = 0$ at the maximum temperature. A boundary condition would be the temperature at any other point Z. The numerical solution of Eq. (1) using these two initial conditions and a boundary condition is designated here as the 2-point method. The development of the procedure to obtain conductivity values using the 2-point method was described in a previous report[2].

Almost all direct electrical heating methods developed heretofore use the central portion of the sample. These methods suffer from the disadvantage that most of the heat generated near the center of the sample is lost by radiation from the surface and only a small fraction is conducted towards the ends. The conductivity is determined from the difference between the rate of energy generated by Joulean heating and rate of energy lost by radiation. Thus, the errors in computing the conductivity are often greater than the errors associated with losses. For example, at a distance of 0.58 cm from the center of a 7" tantalum sample used in the present investigation,

the rate of heat generation was 95.784 W cm^{-3} and the rate of energy lost by radiation (assuming a total hemispherical emittance of 0.184) was 90.060 Wcm^{-3}. Thus, the rate conducted was only about 5% of the energy generated at this location. If the emittance value was in error by 1%, this would lead to an error in the conduction term of 16%. At a distance of 1.94 cm from the center, 10% of the energy is conducted. At this location, a 1% error in emittance leads to a 9% error in the conduction term.

This example demonstrates the advantage of using data away from the sample center. Methods developed in the past by other investigators could not utilize this advantage because they could not solve the second order non-linear differential equation without making mathematical assumptions which are valid only near the center of the sample. However, the development of the analytical techniques detailed in a previous report[2] makes it possible to include some temperature data away from the sample center and significantly increases the accuracy and applicability of direct electrical heating methods.

A method which utilizes only data measured away from the sample center would not be subjected to large errors due to uncertainties in emittance values. Since it is possible to obtain conductivity values using Eq. (1) and three conditions, a computer program (the 3-point method) which utilizes one initial and two boundary conditions, i.e. the temperature at any three different positions, was developed. The 3-point method has the advantage that it is not necessary to locate the position of maximum temperature precisely, nor does it require the precise measurement of the center temperature which is required for the 2-point method. Thus, it is now possible to compute conductivity values using only data away from the center, only data near the center, or data from both the central and non-central regions.

The 2- and 3-point methods can be used to obtain a large number of conductivity values from a small set of data. For example, 576 separate conductivity values can be computed from a temperature profile consisting of 16 data points. This is in marked contrast to the other methods which yield only one conductivity value and require very restrictive mathematical approximations. Consider the 140 amp, current "up" temperature profile shown in Figure 5 for a 5" long tantalum sample. Thermal conductivity values can be computed using the temperature measured at 11.5, 12.0 and 12.5 cm; at 12.0, 12.5 and 13.0 cm; at 12.0, 13.0 and 14.0 cm; at 12.5, 14.5 and 19.0 cm; etc. Thus, over 600 separate values can be computed from this profile. However, the 3-point method may not yield satisfactory conductivity values when the temperature at three adjacent positions are

used. This is due to the large uncertainty in the temperature profile through three adjacent points when the errors concerning the value at each point are considered, whereas the uncertainty in the temperature profile is much less when the points are sufficiently separated.

The data in Figure 5 also clearly indicate the change in the temperature profile caused by reversing the current flow. It is seen that the temperatures on the left side of the sample are appreciably lower and the temperatures on the right side are appreciably higher when the current flow is in the reversed (down) direction. This is caused by the Thomson Effect and is particularly noticeable for tantalum. Since the temperature gradient is positive on the left side of the sample and negative on the right side, the last term in Eq. (1) will have opposite signs on the two sides of the sample. Also, the quantity I/A comes from the vector $\vec{J}$ and has a positive and negative direction[5]. Thus, reversing the current flow changes the sign of the last term in Eq. (1) and causes large temperature changes at positions away from the center when the direction of current flow is reversed (140 amp, current down). For example, at 12.0 cm the temperature decreased from 1486.6 K to 1424.4 K upon current reversal. This indicates that tantalum has a significant Thomson coefficient. Both the 2-point and 3-point methods can be readily used with Eq. (1) including the Thomson term providing the value of the Thomson coefficient is known.

A typical computer output is shown in Figure 6. The first line describes the sample, general experimental conditions and date experiment was performed. The second and third lines give the coefficients for a polynominal fit to electrical resistivity (RHO) and total hemispherical emittance (E). A is the cross-sectional area, TA is the ambient temperature, I is the current, and PER is the circumference. The temperatures TZ1, TZ2, TZ3 at three positions Z1, Z2 and Z3 are the inputs. MU is the Thomson coefficient. The computed value of thermal conductivity is printed next and the effective temperature of the measurement is printed last. Printed between the conductivity value and effective temperature are computed temperatures at various positions, first temperature derivative with respect to position (T≠Z) and the relative magnitude of the terms concerned with heat conduction, generation, radiation and Thomson heating and cooling.

It should be noted that this computer procedure involves starting with an initial condition. In Figure 6, this condition is 1932.2 K at 14.00 cm. Using Eq. (1), initial guesses for λ and dT/dZ, and the shooting technique discussed in a previous report[2] a temperature at Z(2) is obtained. The value of the computed temperature at Z(2) is compared to the measured temperature at Z(2). Based upon the difference between

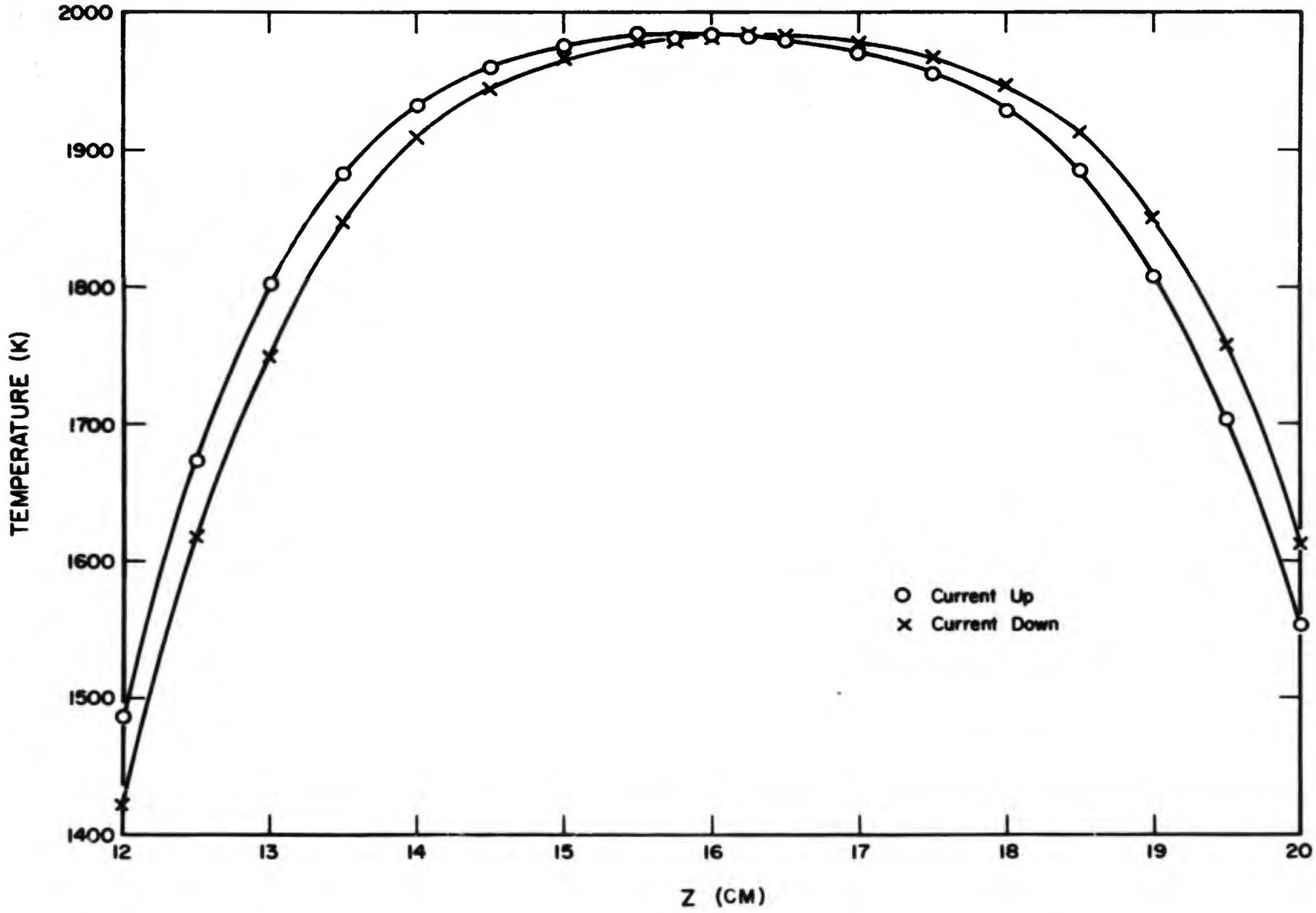

FIGURE 5 TEMPERATURE PROFILES FOR TANTALUM (140 AMPS, 5" SAMPLE)

Note: Reverse page 18 is blank.

TANTALUM 140 AMP UP 5 INCH SAMPLE 11-29-68

RHO = 4.4363300E-06 4.1944200E-08-2.3220000E-12

E = 5.3107200E-02 5.3865500E-05 1.7989600E-08

A = 7.2355200E-02 TA = 2.9020000E+02

I = 1.4016087E+02 PER = 1.0030404E+00

TZ1 = 1.9322192E+03 Z1 = 1.4000000E+01

TZ2 = 1.8025224E+03 Z2 = 1.3000000E+01

TZ3 = 1.4865786E+03 Z3 = 1.2000000E+01

MU = +3.0000000E-05

THERMAL CONDUCTIVITY IS .60488

TEMPERATURE PROFILE

Z	T(Z)	T*(Z)	CONDUCTION	HEATING	RADIATION	THOMPSON
14.0000	1932.22	76.034	46.990	288.235	245.664	-4.419
13.9000	1924.21	84.177	51.585	287.243	240.550	-4.892
13.8000	1915.36	93.110	56.559	286.145	234.998	-5.411
13.7000	1905.56	102.899	61.929	284.930	228.982	-5.980
13.6000	1894.75	113.608	67.704	283.586	222.485	-6.603
13.5000	1882.81	125.306	73.890	282.100	215.492	-7.283
13.4000	1869.65	138.061	80.489	280.459	207.994	-8.024
13.3000	1855.16	151.940	87.492	278.648	199.987	-8.830
13.2000	1839.22	167.010	94.884	276.653	191.474	-9.706
13.1000	1821.72	183.332	102.641	274.456	182.470	-10.655
13.0000	1802.51	200.964	110.723	272.040	172.996	-11.679
12.9000	1781.48	219.956	119.083	269.386	163.086	-12.783
12.8000	1758.48	240.348	127.655	266.475	152.788	-13.968
12.7000	1733.36	262.170	136.361	263.286	142.161	-15.236
12.6000	1705.99	285.436	145.108	259.798	131.279	-16.589
12.5000	1676.23	310.144	153.786	255.990	120.229	-18.024
12.4000	1643.92	336.273	162.271	251.840	109.111	-19.543
12.3000	1608.93	363.779	170.429	247.324	98.036	-21.141
12.2000	1571.12	392.598	178.114	242.421	87.123	-22.816
12.1000	1530.37	422.637	185.175	237.108	76.495	-24.562
12.0000	1486.55	453.781	191.458	231.365	66.278	-26.372

EFF T= 1771.5

FIGURE 6. TYPICAL COMPUTER OUTPUT (3-POINT METHOD)

Note: Reverse page 20 is blank.

computed and measured temperatures, new values of dT/dZ are tried. The procedure is repeated until the computed temperature at Z(2) closely matches the measured temperature. Then the procedure is continued over the range from Z(1) to Z(3) adjusting the value of λ until the computed temperatures at both Z(2) and Z(3) closely approach the observed values. In the case illustrated in Figure 6, the computed values at Z(2) and Z(3) are 1802.51 and 1486.6 K while the measured temperatures are 1802.5 and 1486.6 K respectively.

In addition to closely matching the temperatures at two other locations, the computer output has listed a great deal of interesting and useful information. The temperatures at other locations are computed and these may be compared to measured temperatures which were not used in this particular computer calculation. For example, in Figure 6 the temperature at 13.5 cm was computed to be 1882.8 K while the measured temperature (Figure 5) was 1882.4 K.

Other computer output information of particular interest are the relative magnitudes of the Joulean, radiation, Thomson and conduction terms at various locations. From Figure 6, we see that the rate of heat conduction is 82% of the rate of heat generation at 12.0 cm. This location is well away from the sample center (Figure 5). However, the rate of heat conduction is only 16% of the rate of heat generation at 14.0 cm which is near the sample center. We also note that if the Thomson coefficient is 30 $\mu V\ K^{-1}$, the Thomson term is about 10% of the conduction term at all locations. Thus, a reasonable knowledge of the Thomson coefficient is required in order to obtain accurate conductivity values using the mathematical techniques discussed so far. Since none of the previous direct heating conductivity methods has included the Thomson term, the results using these methods must be in error for materials whose Thomson coefficient approaches that of tantalum (providing DC current was employed in the measurements). DC current is preferred over AC current experimentally because the regulation is much better and phase shift problems do not exist. It should be emphasized that the Thomson Effect is not eliminated in DC measurements by averaging the temperature profiles obtained with the current flow in both directions. Such a procedure will cause the computed conductivity value to be high (neglecting other errors). One should average the differential equations and not the temperature distributions, which are related to the differential equations in a complicated fashion.

Both the 2- and 3-point methods as presented so far have two drawbacks: (1) a value of the Thomson coefficient is required for accurate conductivity values and (2) each conductivity value depends on only two or three specific data points. Although these two methods can be used to obtain a large number of conductivity

values from a small set of data, the two drawbacks cause these computed conductivity values to be scattered. Even when a reasonable value of the Thomson coefficient is used and computed values from adjacent data points are ignored, the scatter band may be ±10%.

Several procedures for computing the Thomson coefficient from the data and for significantly reducing the scatter band have been worked out. One procedure involves the assumption that the values of dT/dZ obtained by the computer using the shooting method are independent of the Thomson coefficient used in the calculation. The validity of this assumption has been tested. A typical example for a set of data in which the value of the Thomson coefficient (μ) was varied are tabulated in Table I.

TABLE I

EFFECT ON dT/dZ CAUSED BY USING DIFFERENT THOMSON COEFFICIENTS

$\mu(10^{-6}$ V $K^{-1})$	dT/dZ (K cm^{-1})
-100	-141.3
0	-142.2
30	-142.6

Thus, it is possible to utilize the various computer outputs which use different data points to construct a graph of dT/dZ versus Z. A plot of dT/dZ versus Z for the 140 amp (switch up) profile on tantalum is shown in Figures 7 and 8. These figures show dT/dZ calculated from a number of runs using different data points (different runs are indicated by different plotting symbols). Data from the lower half of the sample are given in Figure 7 and data from the upper half are shown in Figure 8. Data from the central portion (Z = 15 to 17) is shown on both figures to provide an overlap. It can be seen that values of dT/dZ obtained from different data points are in excellent agreement. Thus, the smooth line drawn through these data is derived from all the experimental data instead of being related to only two or three data points. Figure 9 contains a plot (□) of the slopes of the curves given in Figures 7 and 8, i. e. it is d^2T/dZ^2. The values so plotted were obtained from Figures 7 and 8 using a straight edge.

Once values of dT/dZ and d^2T/dZ^2 are known for a particular temperature, it is possible to calculate λ and μ at that temperature. For example, from the curves of Figures 7 to 9, and from similar curves for 130 amps, the following values were obtained for tantalum at 1844.9 K.

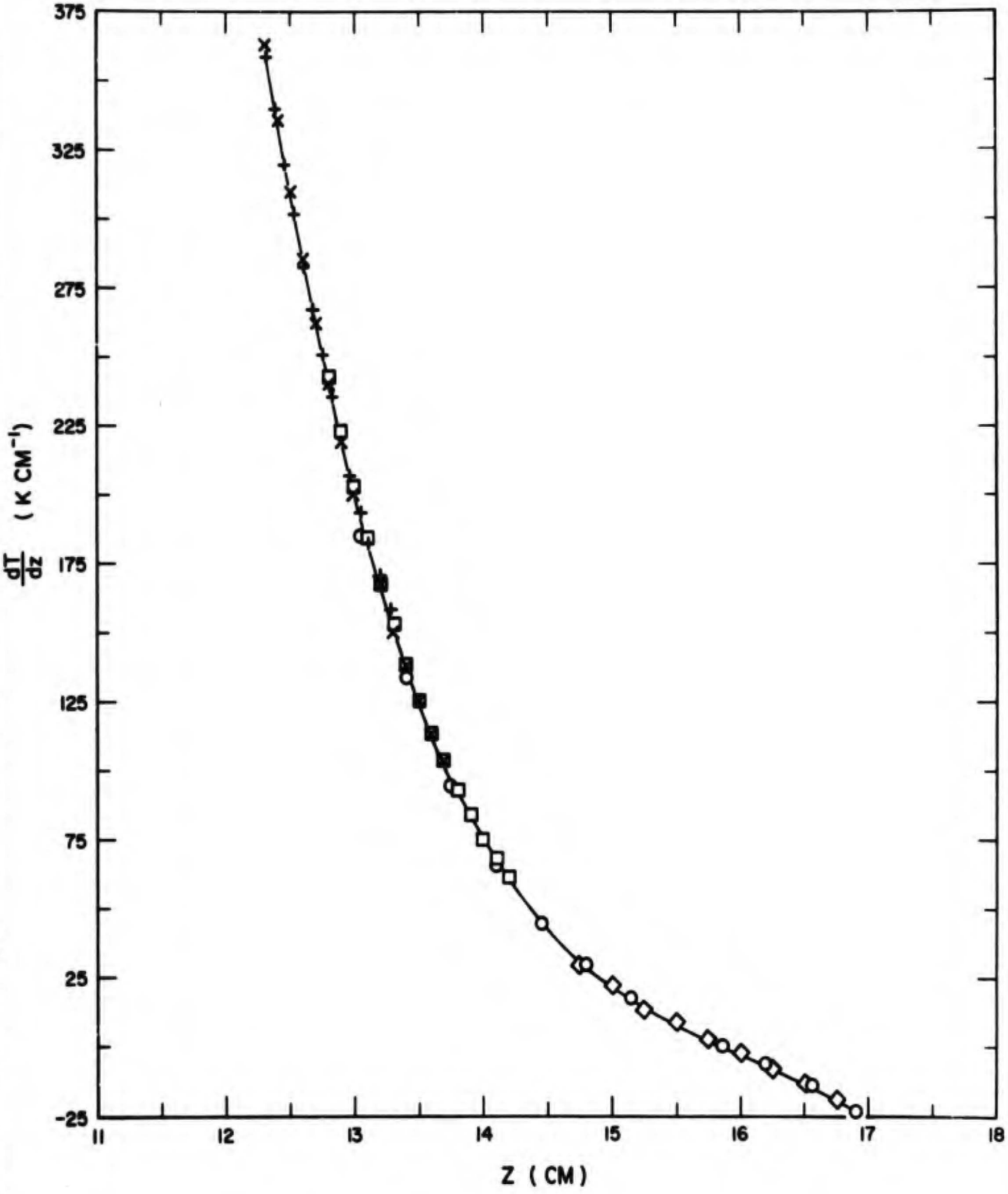

FIGURE 7 dT/dz FROM LOWER PORTION OF TEMPERATURE PROFILE (140 AMP UP, TANTALUM)

Note: Reverse page 24 is blank.

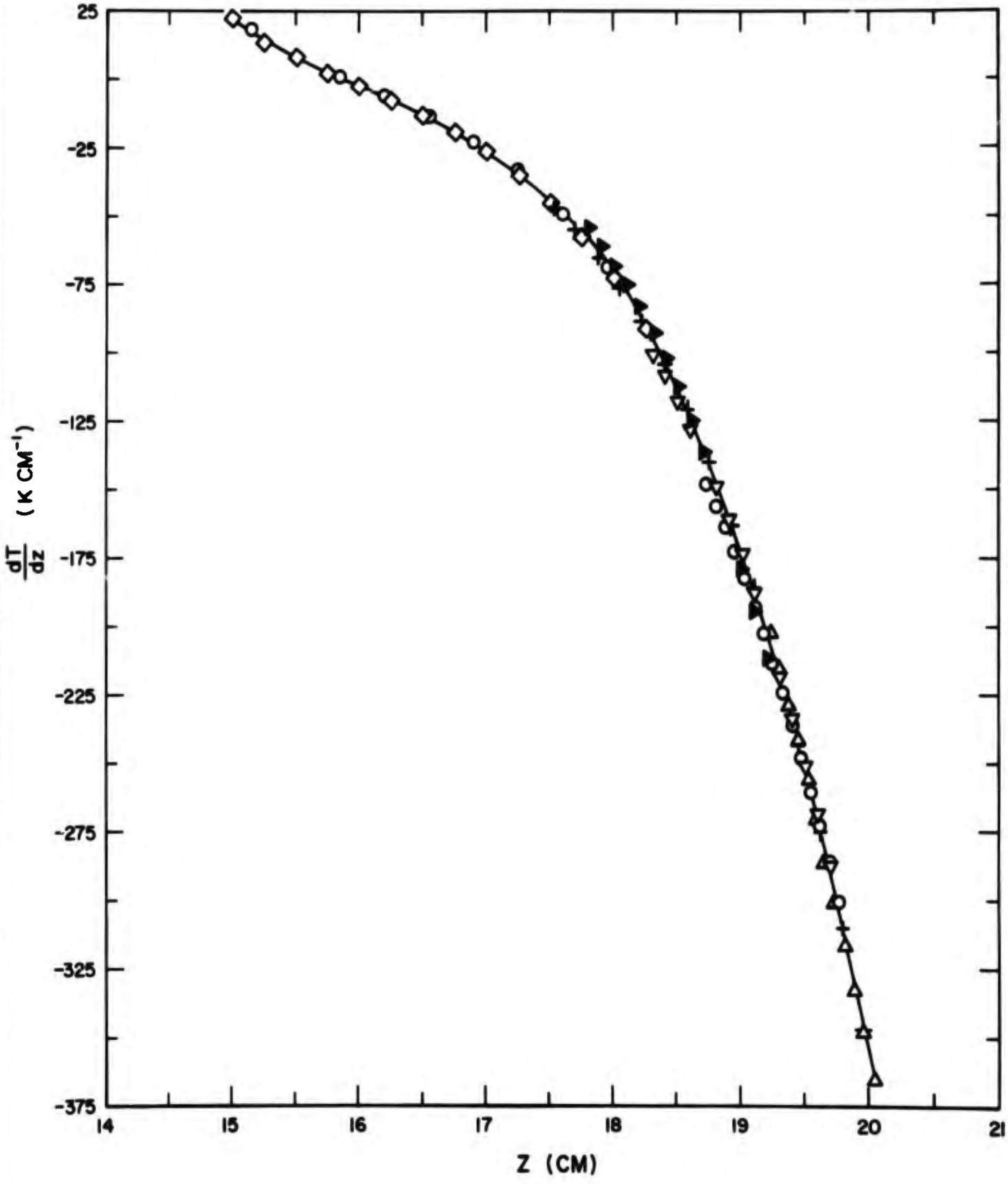

FIGURE 8 dT/dz FROM UPPER PORTION OF TEMPERATURE PROFILE (140 AMP UP, TANTALUM)

Note: Reverse page 26 is blank.

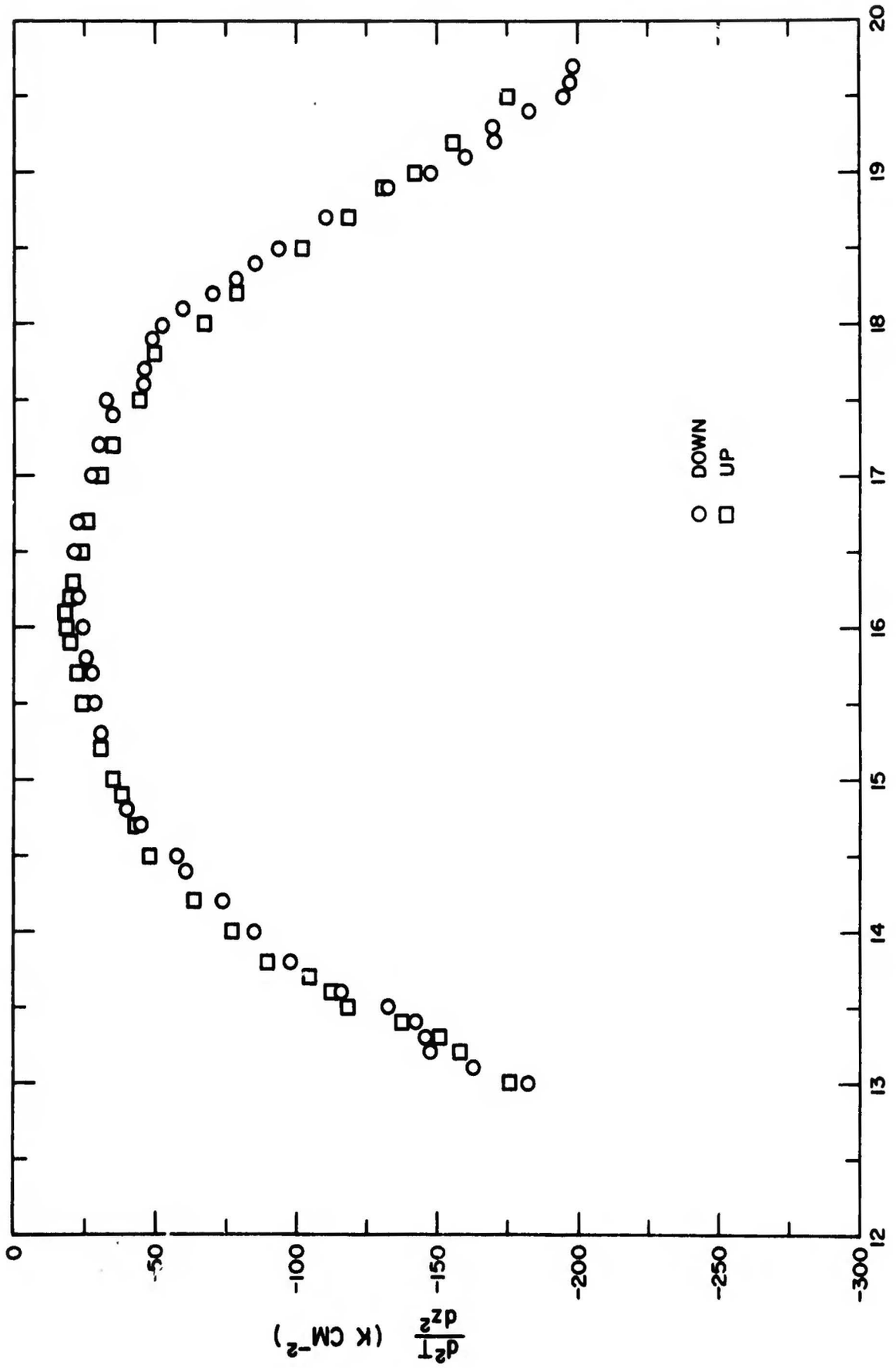

FIGURE 9 DERIVATIVE OF dT/dz PLOTS (140 AMP PROFILE, TANTALUM)

Note: Reverse page 28 is blank.

TABLE II

VALUES OF dT/dZ AND d^2T/dZ^2 AT 1844.9 K

Current	dT/dZ (K cm^{-1})	d^2T/dZ^2 (K cm^{-2})	F (W cm^{-3})
140 amps up	-143	-119	82.740
140 amps down	-153	-148	82.740
130 amps up	- 75	- 66	45.300
130 amps down	- 80	- 77	45.300

F is the difference between the terms for generated and radiated power (i.e. $I^2\rho/A^2 - P\epsilon_H\sigma(T^4 - T_0^4)/A$]. From Eq. (1) we obtain

$$\lambda d^2T/dZ^2 - \mu(I/A)(dT/dZ) = -F$$

From the data obtained with the current flow down and up, we obtain several simultaneous equations such as:

$$\lambda(-148) - \mu(140/.07235)(-153) = -82.740$$

$$\lambda(-119) - \mu(-140/.07235)(-143) = -82.740$$

Using the data in Table II, six values of λ and μ were determined. These are listed in Table III.

TABLE III

THERMAL CONDUCTIVITY AND THOMSON COEFFICIENTS CALCULATED FOR TANTALUM AT 1844.9 K

λ(W cm^{-1} K^{-1})	μ(10^{-6}V K^{-1})	Condition*	
0.6220	31.46	140↓	140↑
0.6225	31.20	130↓	130↑
0.6220	31.44	140↓	130↑
0.6225	31.24	140↑	130↓
0.6312	36.65	140↓	130↓
0.6214	31.75	140↑	130↑

*140↓ refers to 140 amps flowing in the down direction.

The results of the last two sets of calculations listed in Table III are relatively less reliable because when the current flow for both equations is in the same direction, it is necessary to subtract two terms of almost equal magnitude in order to obtain the conductivity. The above procedure markedly reduces the scatter in λ values and simultaneously yields a value for the Thomson coefficient. Furthermore, these calculations are based on results obtained for the same temperature, i.e., the temperature assigned to the λ and μ values is uniquely defined without any averaging techniques. This procedure has not been computerized, but there appears to be no problems in doing so, with the exception that the computer cost per run may become significant. The computer cost for obtaining each conductivity value by the 2- or 3-point method is less than 10 cents.

A procedure for determining one value of conductivity and Thomson coefficient per profile is under development. This approach involves using a spline fit[6] to obtain reasonable agreement with the entire experimental temperature profile. The spline fit is chosen so that the second temperature derivative is continuous. The fit is then differentiated twice and the best values of conductivity and Thomson coefficient are obtained using a least squares routine. This approach is relatively rapid and involves no assumptions. Values of the Thomson coefficient can be obtained using only one profile and the current need not be reversed. The optimum number of knots used in the spline fit can readily be determined and can be varied by one or two knots without significantly altering the results. In addition, the program permits both the thermal conductivity and Thomson coefficient to be either fixed or variable. For example, using a 140 amp profile on tantalum the values given in Table IV are obtained.

TABLE IV

THERMAL CONDUCTIVITY AND THOMSON COEFFICIENTS FOR TANTALUM AT 1700 K

Fixed	Variable	5 Knots		6 Knots	
		λ ($W\,cm^{-1}K^{-1}$)	$\mu x10^6$ ($V\,K^{-1}$)	λ ($W\,cm^{-1}K^{-1}$)	$\mu x10^6$ ($V\,K^{-1}$)
$\lambda;\mu$		0.6440	37.0	0.6431	38.0
λ	μ	0.6439	37.2	0.6436	38.4
μ	λ	0.6393	40.1	0.6384	41.8
	$\lambda;\mu$	0.6411	37.9	0.6406	39.2

Both procedures considerably reduce the scatter band on conductivity values and provide values for the Thomson coefficient. It is very significant that all conductivity values for tantalum obtained by procedures utilizing the entire profile have always been within 5% of the recommended curve[7], whereas some calculations of conductivity based on 2- or 3-point methods have been more than 20% from the recommended curve. Thus, the two procedures outlined above considerably reduce the scatter band and increase accuracy of the conductivity values.

III. EXPERIMENTAL RESULTS AND DISCUSSION

A. Tantalum

1. Sample Description

The results of thermal conductivity measurements on stainless steel and molybdenum are detailed in a previous report[2]. The results on stainless steel were quite satisfactory. However, the results on molybdenum were poor, mainly due to the use of samples consisting of thin-walled tubing (0.125" OD with a 0.092" ID bore) which permitted significant heat exchange by radiation along the bore. As part of the method evaluation, satisfactory results were desired on a material whose conductivity was appreciably higher than that of stainless steel. Consequently, suitable samples of metallurgical grade thick-walled tantalum tubing were obtained*. The tubes were 0.125" OD with a 0.040" ID bore. The purity was about 99.9 percent with small amounts of silicon, magnesium, copper and calcium and traces of iron, nickel and zirconium present. The density was 16.6 gm cm^{-3}.

2. Electrical Resistivity

The results of electrical resistivity determinations from 300 to 2550 K are shown in Figure 10A. The day-by-day reproducibility is illustrated in Figure 10B, which is a magnified portion of Figure 10A covering the temperature interval from 1050 to 1650 K. From Figure 10B, it is seen that the scatter in the resistivity values is usually less than ±0.2%. The good agreement between the present results and other published results is shown in Figure 11 where data of Taylor and Finch[8], Tye[9], Gumenyuk, Ivanov and Lebedev[10], and Petrov, Chekhovskoi and Sheindlin[11] are plotted along with the smooth curve derived from Figure 10A.

*Uniform Tubes, Inc., Collegeville, Pennsylvania

3. Emittance

Total hemispherical emittance values for tantalum are shown in Figure 12A. Between 1000 and 1400 K, the initial emittance values increased from 0.186 to 0.195. However, after prolonged heating above 2000 K, the emittance values near 1100 K were considerably less than the original values, but they tended to increase with time at constant temperature. It appears that in the temperature range 1000 to 1400 K at 10^{-7} torr, a reversible reaction occurs in which gas is adsorbed or desorbed. This gas adsorption increases the total hemispherical emittance by about 25%. Similar experiences have been reported in the literature[12]. Therefore, it was necessary to age the samples above 2000 K before taking data and to minimize exposing the critical section of the sample to temperatures in the 1000 to 1400 K range. When these precautions were taken, data were reproducible within 1% (Figure 12B). The present total hemispherical emittance results are compared to literature values in Figure 13 in which data of Butler et al.[13], Malter and Langmuir[14], Schwartz[15], Abbott[16] and Peletskii and Voskresenskii[17] are plotted. The reasonably good agreement among the various researchers is noted.

Spectral emittance values (at 0.65 microns) for tantalum are plotted in Figure 14. These data were obtained using an internal platinum/platinum-10% rhodium thermocouple to obtain true temperature. Averaged spectral emittance data[12] of Abbott[16] and Serebryakova, Paderno and Samsonov[18] are also shown in Figure 14. The present data agree with the published results within 2% above 1400 K where surface films have been removed.

4. Thermal Conductivity

Thermal conductivity values were computed from sixteen temperature profiles. Two of these profiles are shown in Figure 5. Experimental conditions used for all profiles are listed in Table V. As discussed in the text, hundreds of conductivity values can be obtained per profile. Therefore, it is not practical to show (or even to calculate) all the conductivity values.

Some of the computed conductivity values obtained from several of the profiles using the 3-point method are shown in Figure 15. Two criteria were used in selecting these conductivity values: (1) the conduction term was greater than 10% of the Joulean heating term over at least two thirds of the portion of the profile used in the calculation and (2) non-adjacent data points were used as input. The values shown in Figure 15 are typical of the values computed when applying these two criteria. We note that the computed values cover a band of about ±13%.

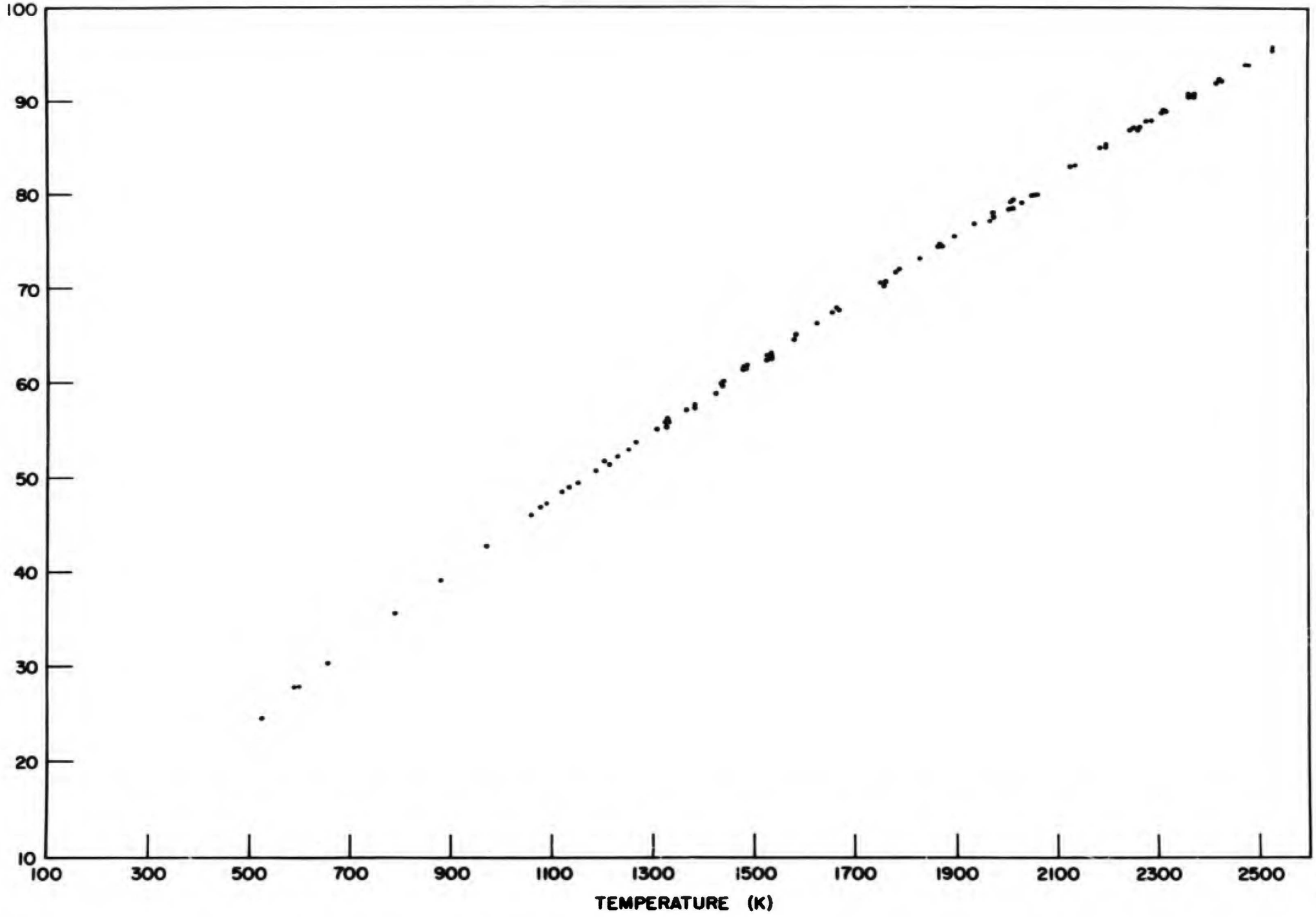

FIGURE 10A. ELECTRICAL RESISTIVITY OF TANTALUM VS TEMPERATURE

Note: Reverse page 34 is blank.

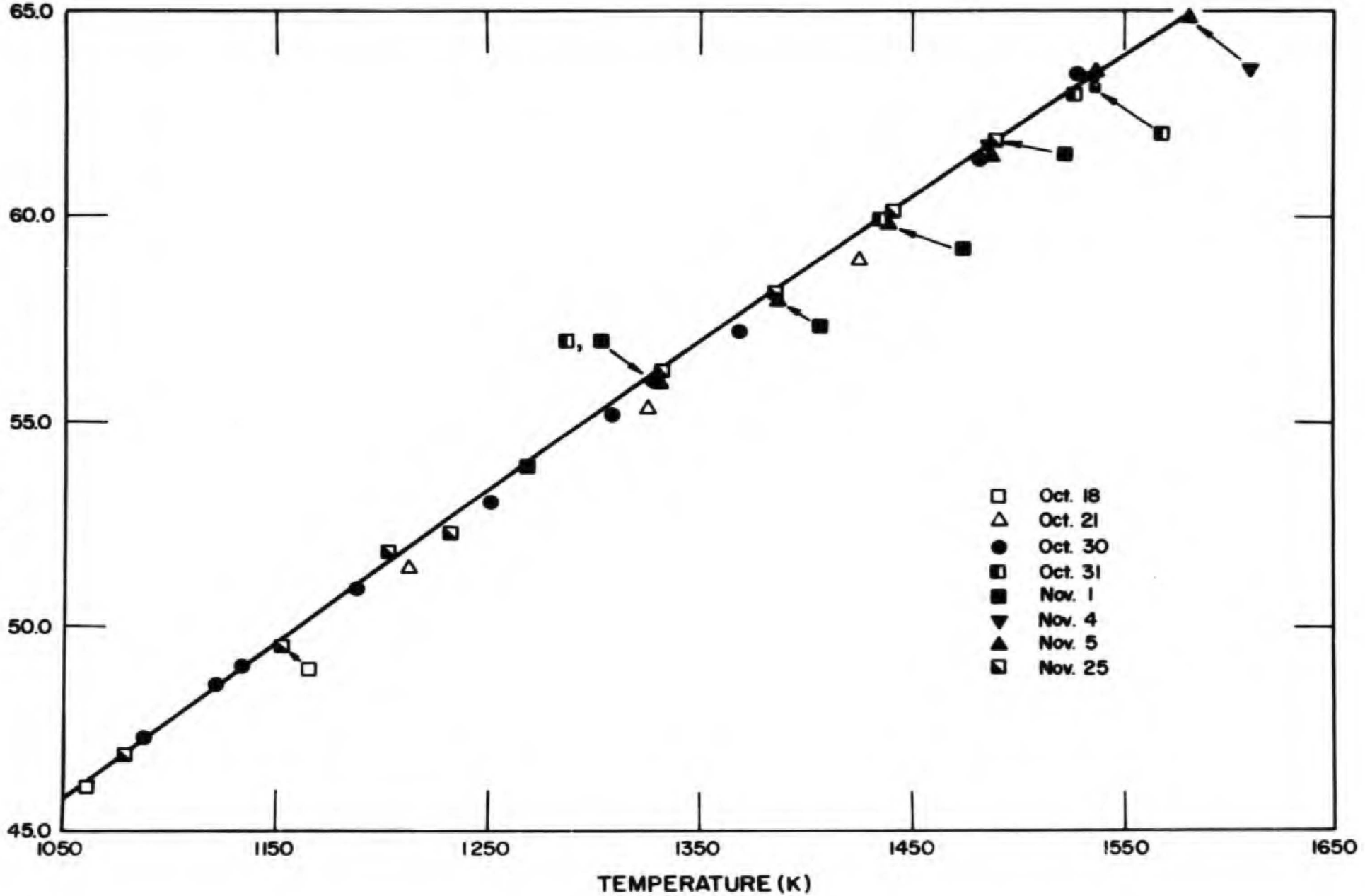

FIGURE 10B ELECTRICAL RESISTIVITY OF TANTALUM

Note: Reverse page 36 is blank.

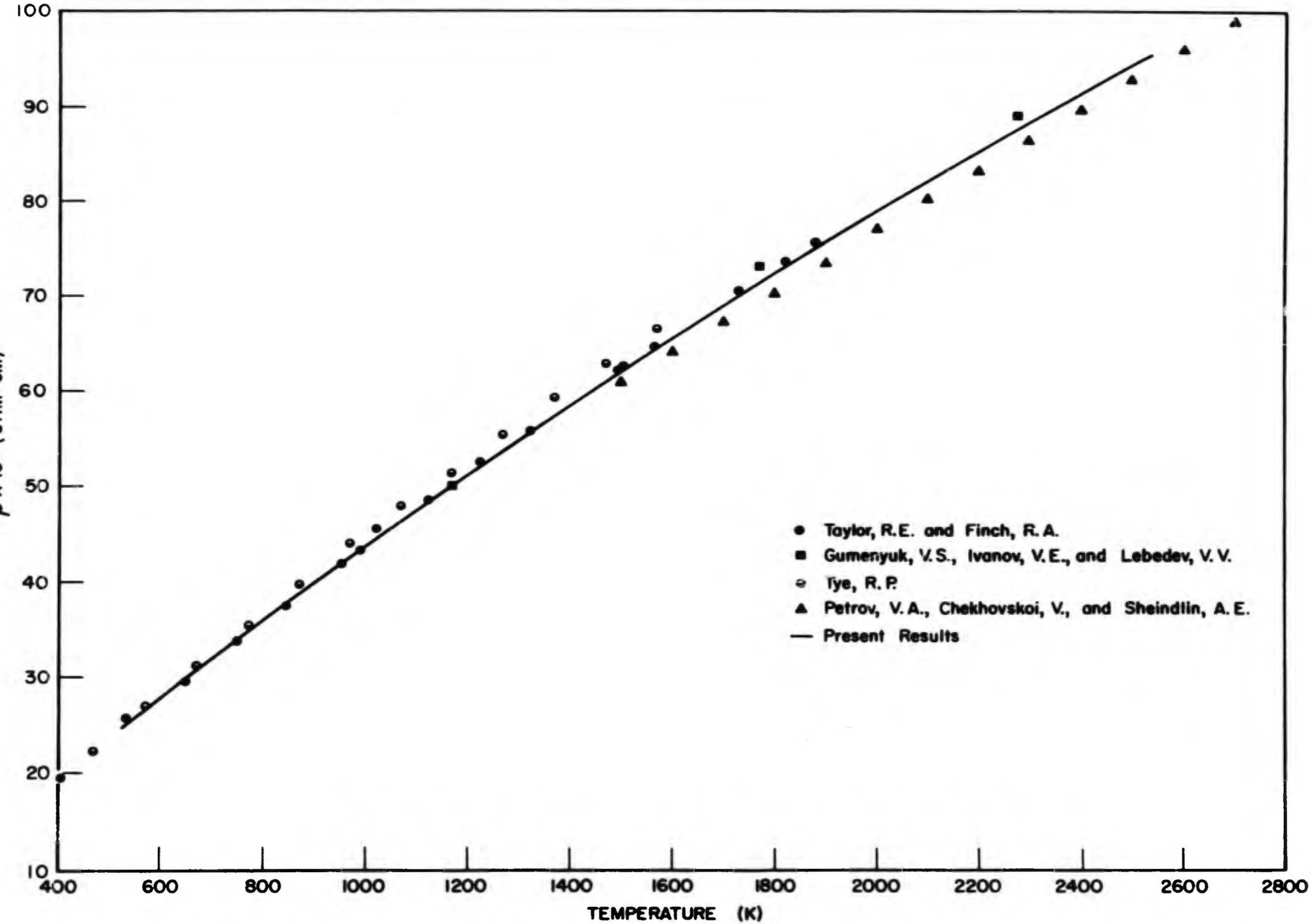

FIGURE 11 COMPARISON OF RESISTIVITY RESULTS WITH PUBLISHED VALUES (TANTALUM)

Note: Reverse page 38 is blank.

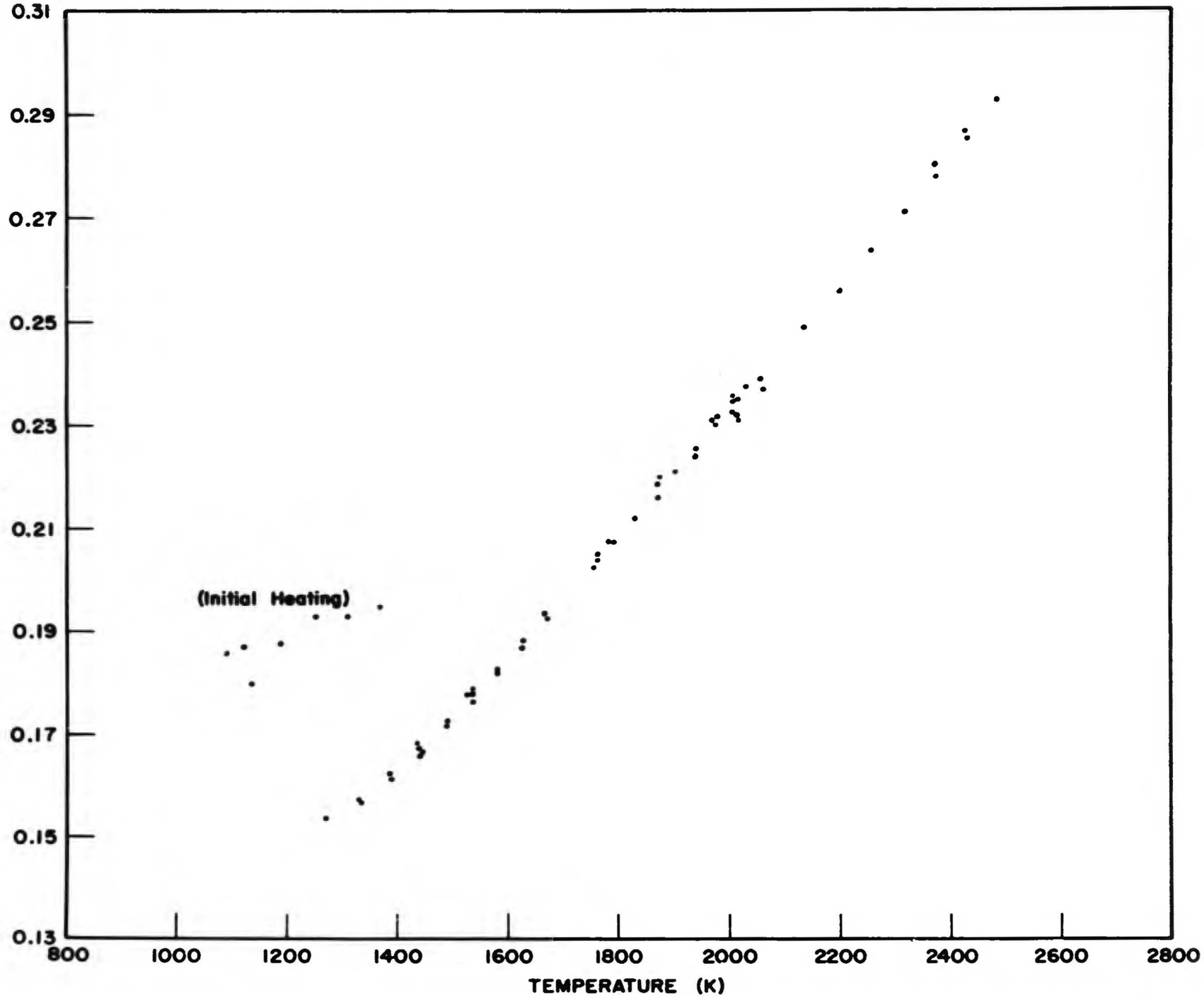

FIGURE 12 A. TOTAL HEMISPHERICAL EMITTANCE OF TANTALUM VS TEMPERATURE

Note: Reverse page 40 is blank.

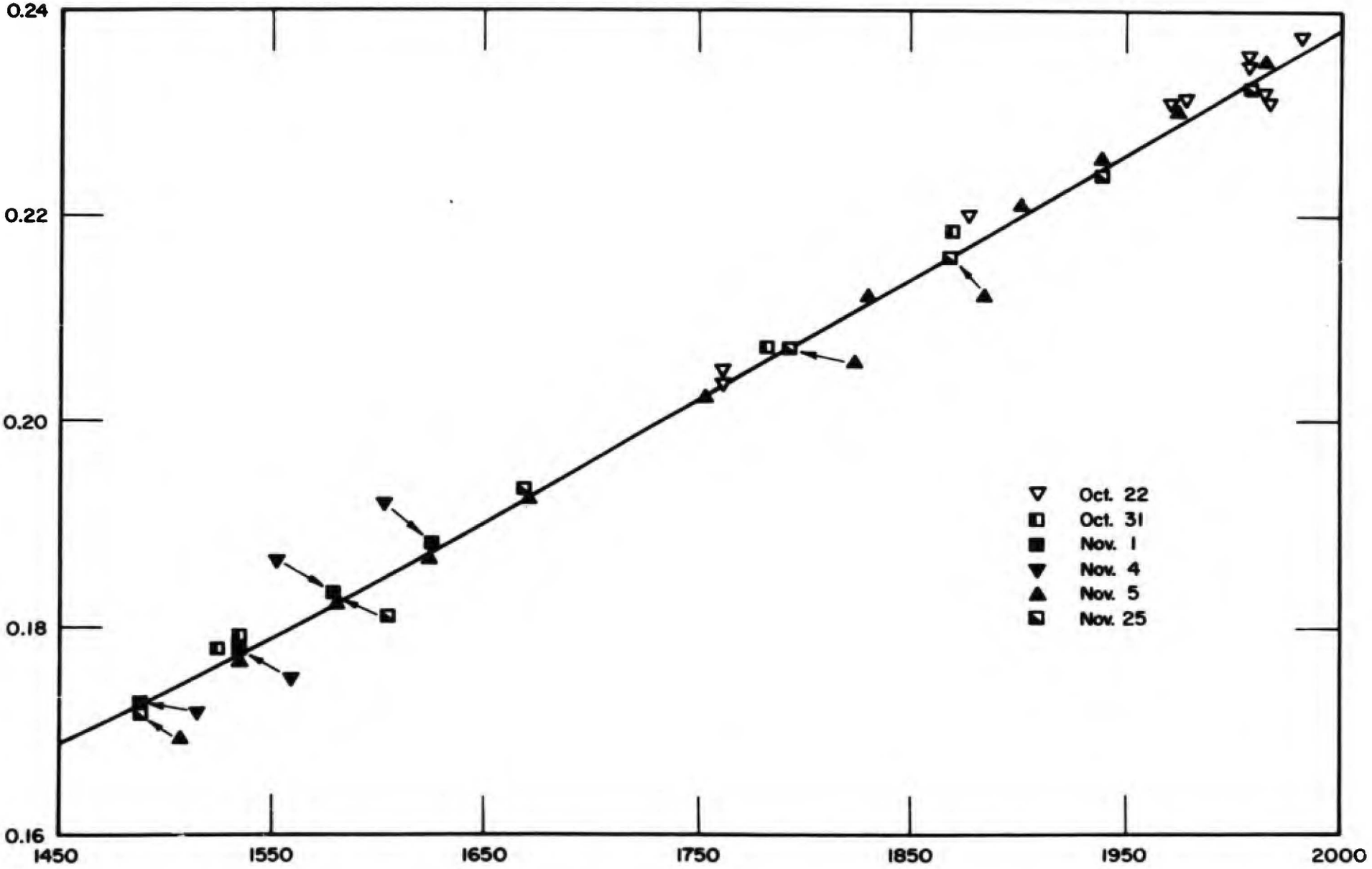

FIGURE 12B. TOTAL HEMISPHERICAL EMITTANCE OF TANTALUM

Note: Reverse page 42 is blank.

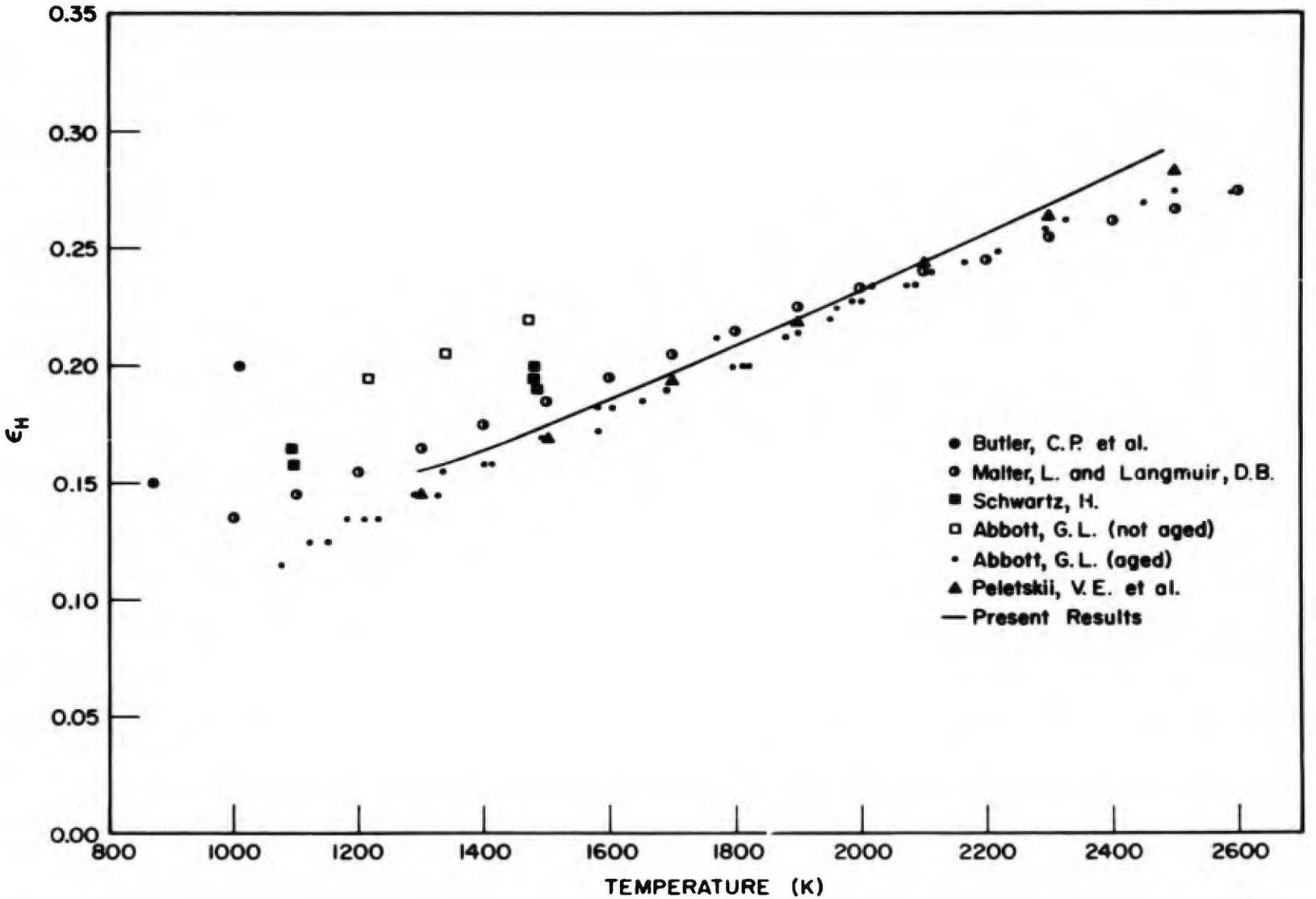

FIGURE 13 COMPARISON OF EMITTANCE RESULTS WITH PUBLISHED VALUES (TANTALUM)

Note: Reverse page 44 is blank.

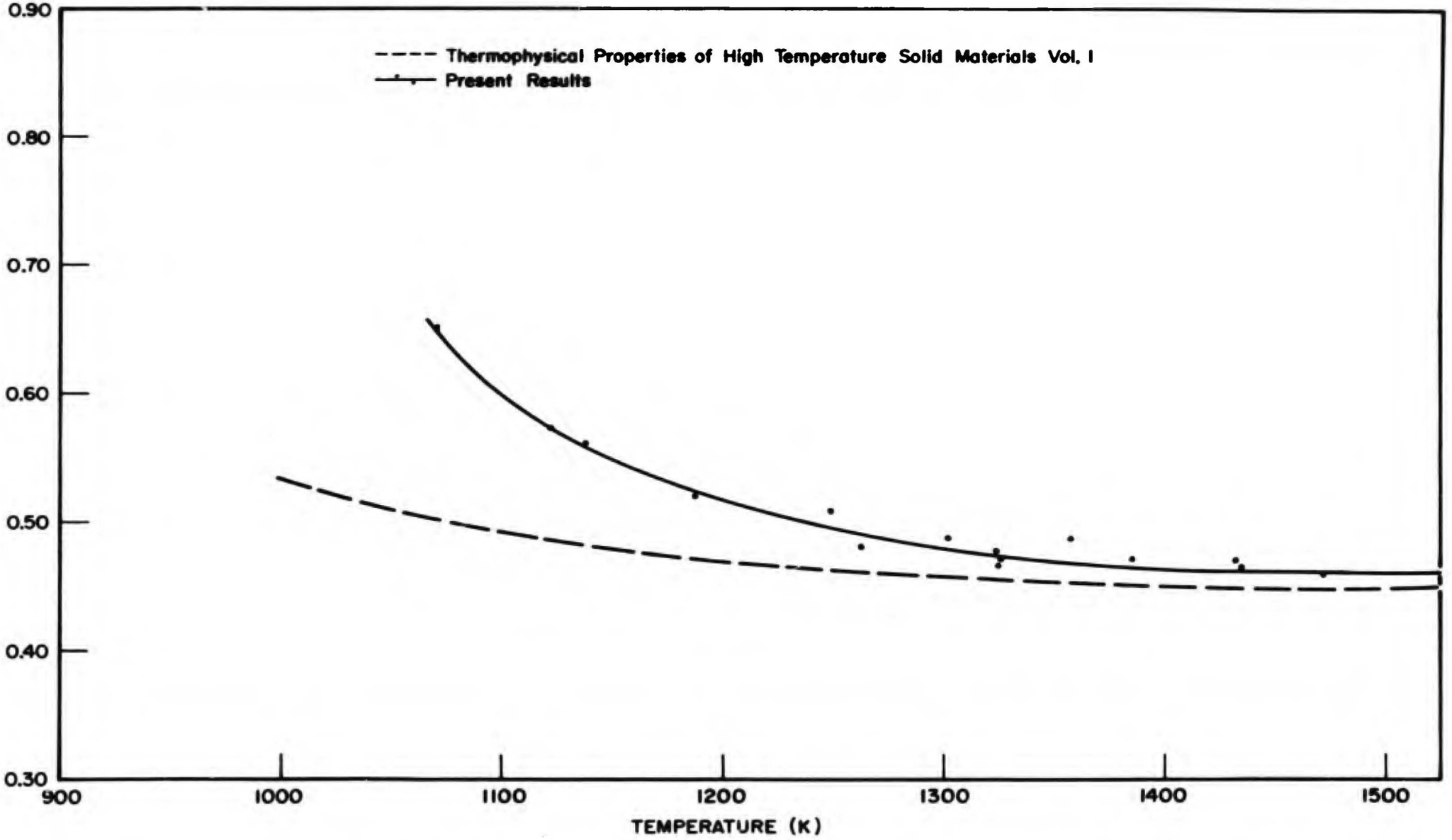

FIGURE 14 SPECTRAL EMITTANCE (0.65 MICRONS) OF TANTALUM

Note: Reverse page 46 is blank.

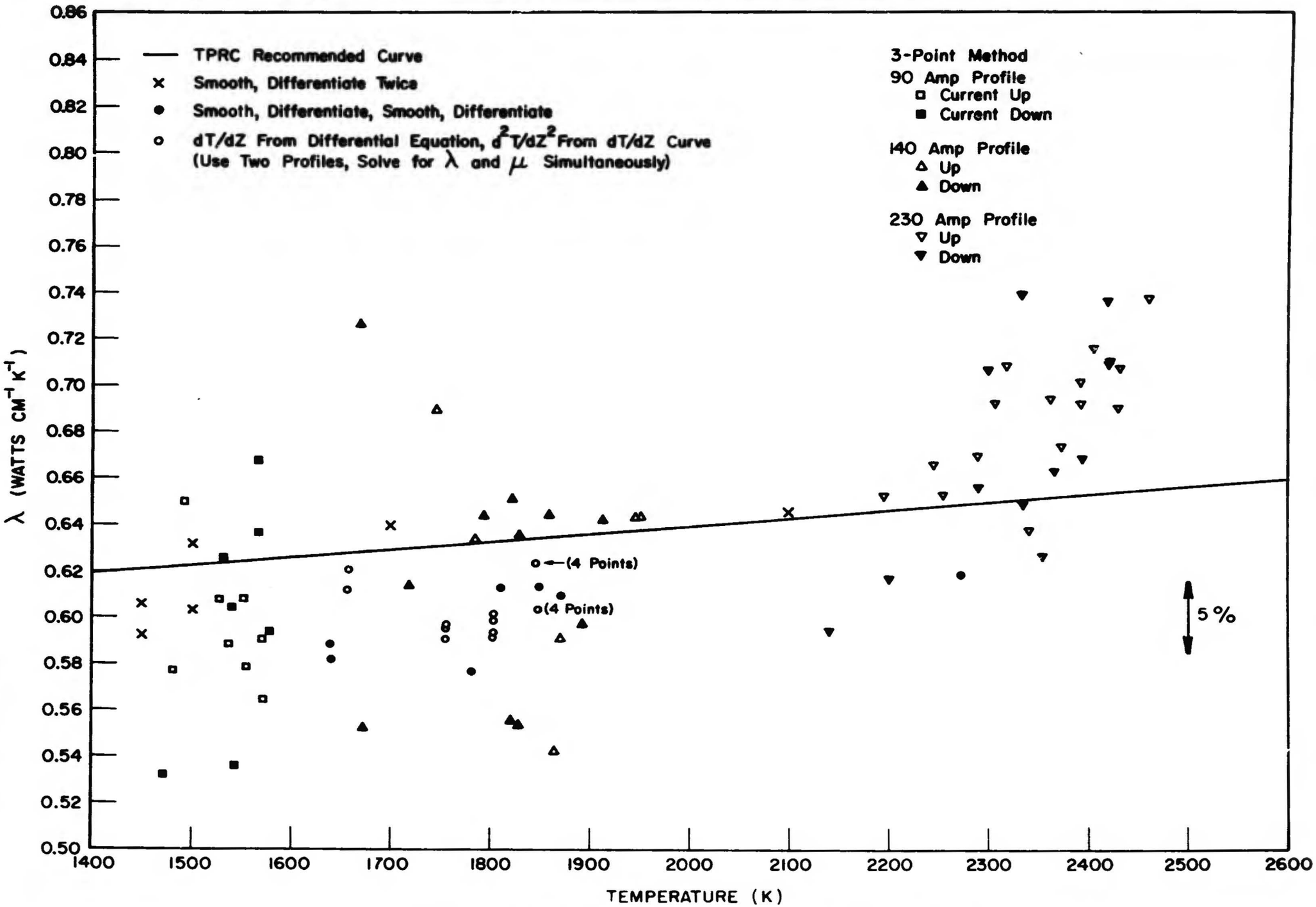

FIGURE 15 THERMAL CONDUCTIVITY OF TANTALUM

Note: Reverse page 48 is blank.

TABLE V

LIST OF TEMPERATURE PROFILES FOR TANTALUM

Current (Amps)	Direction of Current Flow	Effective Length of Sample (inches)	Current (Amps)	Direction of Current Flow	Effective Length of Sample (inches)
80	up and down	7	130	up and down	5
90	"	7	140	"	5
110	"	7	230	"	2.5
110	"	5	270	"	2.5

In addition to the 2- and 3-point methods, we may use techniques which employ more than two or three data points in calculating a thermal conductivity value. Some possible schemes are shown in Figure 16. We may smooth the data (all smoothing operations were performed using spline fits)[6]. We may then differentiate the fits twice to obtain values for dT/dZ and d^2T/dZ^2 for different locations. In general the d^2T/dZ^2 values so obtained may not be very close to the values obtained at each location by other techniques[6]. However, by using a least squares routine, it is possible to compute a conductivity value which is relatively independent of the point-by-point scatter in d^2T/dZ^2 values. Alternately, after smoothing the temperature profiles and differentiating once to obtain dT/dZ, these resulting values are also smoothed and differentiated to obtain d^2T/dZ^2. This alternate procedure yields improved values of d^2T/dZ^2.

A third scheme (mentioned previously) involves using the dT/dZ values obtained from the 3-point method (Figures 7 and 8). It should be emphasized that these values were obtained using Eq. (1) instead of fitting temperature profiles directly. The values for dT/dZ can be smoothed and differentiated once to obtain d^2T/dZ^2. This procedure has yielded excellent results (Table IV), but has not been automated as yet. Consequently, it involves a great deal of effort.

Conductivity values obtained using these three schemes are included in Figure 15. Note that using any of the schemes indicated in Figure 16 reduces the scatter considerably. The recommended curve[7] for the thermal conductivity of tantalum is also shown in Figure 15. The results of techniques which employ more than two or three data points per calculated conductivity value are usually within 5% of the recommended curve. It should be noted this is within the uncertainty associated with the recommended curve. Data of Worthing[19], Rasor and McClelland[20], Allen, Glasier and Jordon[21], Gumenyuk, Ivanov and Lebedev[10], Jun and Hoch[23], and Peletskii and Voskresenskii[17] are shown in Figure 17 along with the recommended curve[7]. The range of present values obtained using the multi-point techniques are indicated by the dashed lines. The present values

were obtained using two assumptions:(1) the conductivity is independent of temperature (this probably causes the results to be 1% low) and (2) energy transport by radiation down the center bore is negligible. The error caused by the latter assumption has not been quantitatively determined, but it increases with increasing temperature and temperature gradient. Subsequent research, including the tungsten and ATJS graphite results reported herein, used solid rods and are not subjected to this error.

Changes in the computed thermal conductivity values for tantalum caused by changing the input parameters are given in Table VI. The changes recorded in Table VI are based on changing only one parameter at a time. This might occur, for example, if ρ were measured on one sample and the temperature profile obtained on another sample. In practice, all data were obtained on the same sample and, due to the principle of superposition, the errors are considerably less than those indicated in Table VI. For example, making a 5 K error in all temperature measurements reduces the error from 4 to about 0.5%. This result emphasizes the need for taking all measurements on the same sample. A complete error analysis has not been completed as yet, but it would appear that accuracies of about 3% in λ values at high temperatures are achievable using direct heating methods on solid rods.

One of the original objectives of this project was the evaluation of the various published direct heating methods. Because of the advances in data handling which have resulted from this program, it is no longer necessary to make the restrictive mathematical approximations inherent in the published techniques. This in effect, renders these methods obsolete. Nevertheless, it was instructive to examine the results which were obtained using these methods and the current data. The data from four profiles (140 amp up and down, 90 amp up and down, Table V) were used in this study.

TABLE VI

EFFECT ON COMPUTED THERMAL CONDUCTIVITY VALUES FOR TANTALUM CAUSED BY CHANGING INPUT PARAMETERS

Parameter	Change in Parameter	Resulting Change in λ
ρ	0.2%	1.0%
ϵ_H	1.0%	4.7%
I	0.2%	2.0%
A	0.4%	3.8%
T	5 K	4%

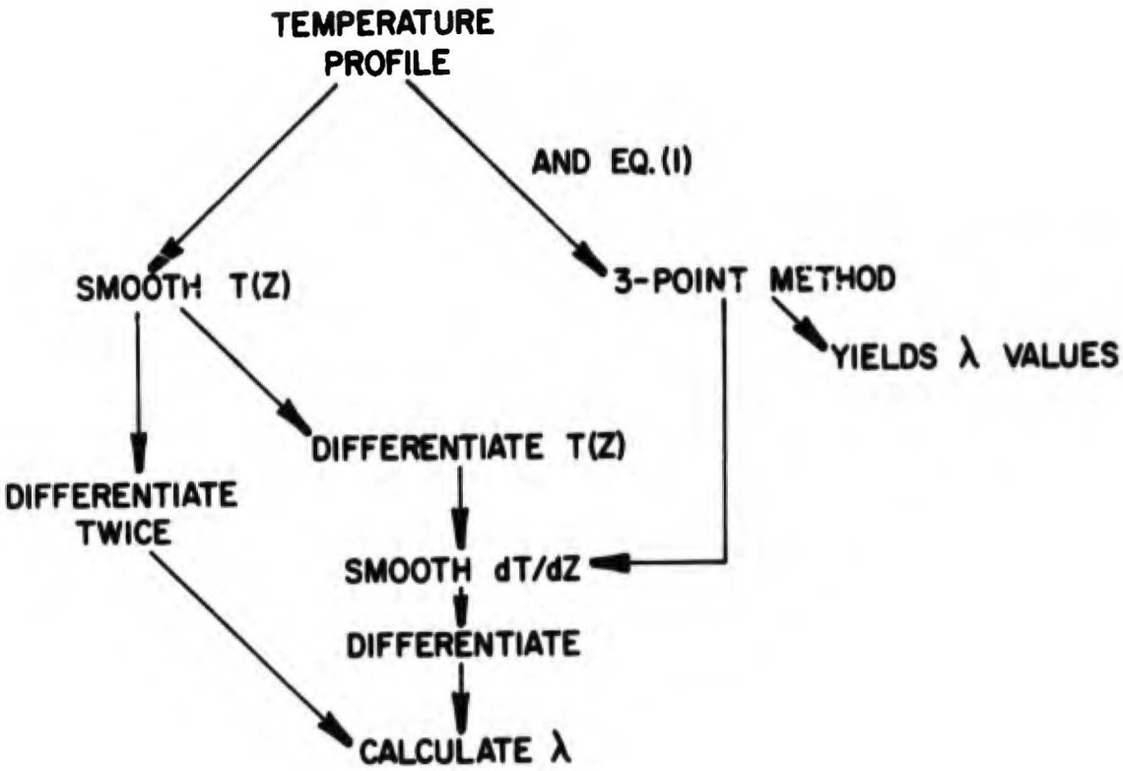

FIGURE 16 COMPUTATIONAL SCHEMES USING MULTIPLE DATA POINTS

Note: Reverse page 52 is blank.

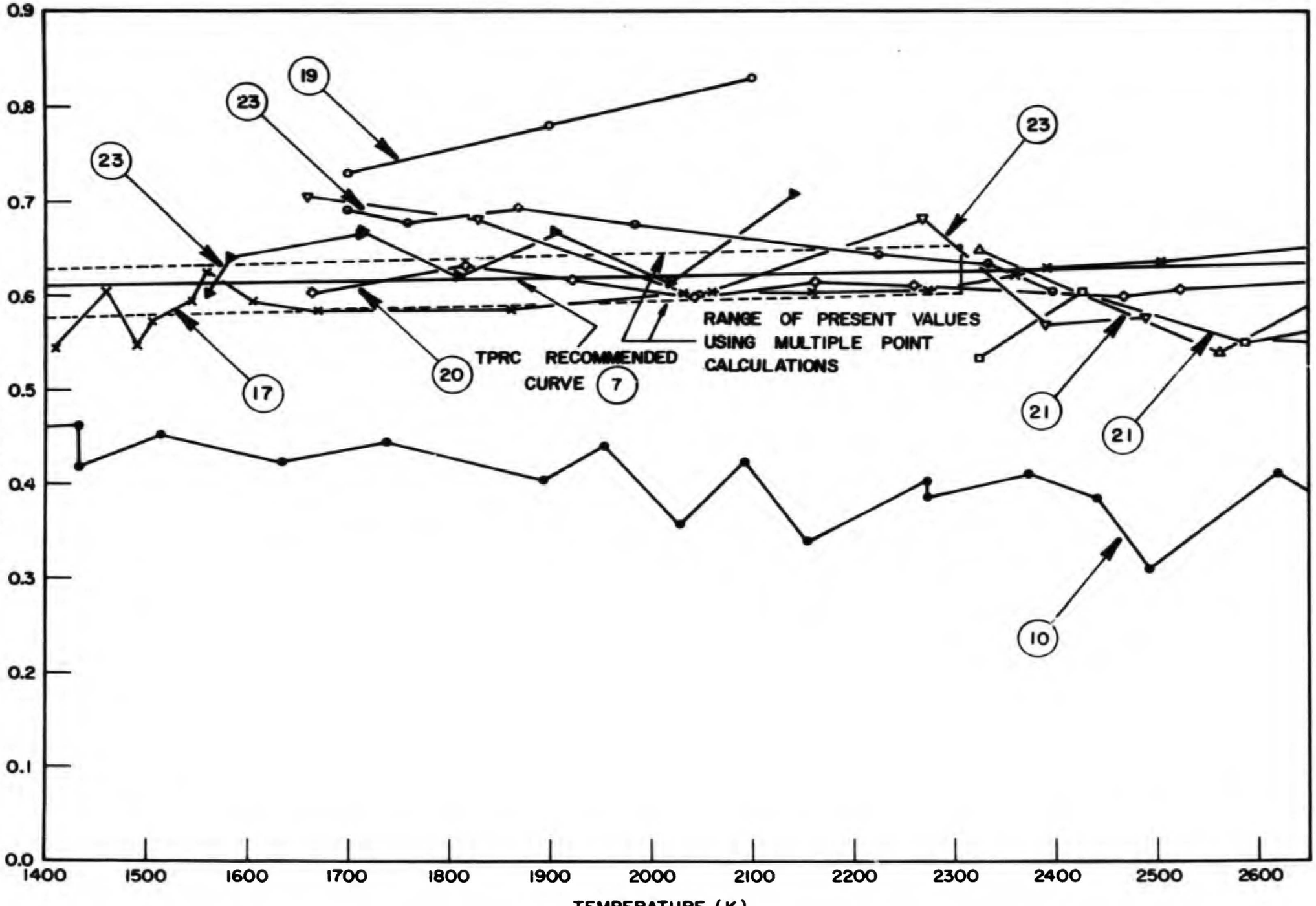

FIGURE 17 PUBLISHED CONDUCTIVITY VALUES FOR TANTALUM

Note: Reverse page 54 is blank.

The equation used to compute thermal conductivity for the Krishnan and Jain method in the parabolic region[1] is

$$(\lambda)_{T_c} = \left(\frac{P\epsilon_H\sigma}{A}\right)_{T_c} \frac{Z^2}{2}\left(\frac{T_\infty^4 - T_c^4}{T_c - T}\right) \qquad \text{Eq. (2)}$$

where T_c is the center temperature of the profile and T_∞ is the temperature which an infinitely long sample would attain if heated with the same current. The quantity $(P\epsilon_H\sigma/A)_{T_c}$ is readily evaluated from the experimental data (ϵ_H vs T, Figures 12A and 12B). In order to evaluate the quantity $Z^2/(T_c - T)$, it is necessary to locate the position of maximum temperature where Z is defined equal to zero in Eq. (2). This is relatively difficult to do even for fairly peaked profiles such as the 140 amp profiles (Figure 5) and is virtually impossible for flattened profiles (90 amp profiles, Figure 18). Since flattened profiles are not parabolic, Eq. (2) is not valid. This case is discussed separately later.

The best procedure for deciding the location of Z = 0 is to plot dT/dZ versus position and determine the point where dT/dZ = 0 (Figures 7 and 8) and redefine this value of Z as zero. However, these values of dT/dZ were obtained from the 3-point method and presumably would not be available for someone using the Krishnan and Jain or Lebedev methods. If they were available, there would be no need to use the Krishnan and Jain or Lebedev techniques. It is possible to plot Z vs $(T_c - T)$ for both positive and negative values of Z, yielding two values of $Z^2/(T_c - T)$ for each profile. The quantity T_∞ is obtained from the long sample data.

The results for the 140 amp profiles (T_c = 1984.8 K) are given in Table VII.

TABLE VII

CONDUCTIVITY VALUES FOR TANTALUM CALCULATED USING THE KRISHNAN AND JAIN AND THE LEBEDEV METHODS (140 amp profile, T_c = 1984.8 K)

Profile	λ(W cm^{-1} K^{-1})	
	Krishnan and Jain	Lebedev
140 Amp Up		
Z positive	0.657	0.663
Z negative	0.688	0.694
140 Amp Down		
Z positive	0.694	0.709
Z negative	0.780	0.790

With one exception, these values are within 10% of the recommended value (0.64 W $cm^{-1} K^{-1}$)[7]. Considering the fact that the Thomson effect has been neglected, these results are good.

Equation (2) is not valid for flattened profiles such as the ones shown in Figure 18. For these cases, the equation

$$\lambda = \frac{4P\epsilon_H \sigma T_\infty^3}{\beta A} \qquad \text{Eq. (3)}$$

is used where β is a constant which is determined graphically[1]. Using this equation and data obtained from the 90 amp up profile, values of 0.559 and 0.426 W $cm^{-1}K^{-1}$ were obtained at 1620 K. The recommended value is 0.626 W $cm^{-1}K^{-1}$. Equation (3) uses data away from the center. Since the Thomson term forces the profile to be non-symmetrical, different values of λ must be calculated from the two sides of the profile.

The equation used to calculate thermal conductivity for the Lebedev method is[1]

$$\lambda = \rho \frac{(I_s^2 - I_\infty^2)}{2A^2 \Delta T} Z^2 \qquad \text{Eq. (4)}$$

where I_s is the current through the short sample and I_∞ is the current required to attain the same temperature in a long sample. Using Eq. (4) and the data from the 140 amp profile, the values given in Table VII were obtained. Because of the $Z^2/\Delta T$ relation, Eq. (4) is not valid for flattened profiles such as the ones shown in Figure 18, except possibly in the central region. Even there the results are not reliable because I_s is nearly equal to I_∞. For example, for the 90 amp profile, I_s = 90.09 amps and I_∞ = 89.00 ± .05 amps. Thus the uncertainty in $(I_s^2 - I_\infty^2)$ is large. Computed conductivity values using the Lebedev method and the 90 amp profile ranged from 0.3 to 0.6 W $cm^{-1}K^{-1}$ compared to values of 0.59 to 0.61 W $cm^{-1}K^{-1}$ using the multiple point programs. Included in Figure 17 are conductivity values for tantalum obtained by Gumenyuk, Ivanov and Lebedev[10]. It is interesting to note that the results of these researches are much lower than the present results using the Lebedev method (or the other methods) even though the electrical resistivity values for the two sets of samples were in close agreement (Figure 11).

Another method for computing the conductivity is Worthing's method[1]. Worthing's method involves graphical integration of the Joulean and radiation terms and subtraction of these terms to determine the conduction term. Rudkin, Parker, Westover and Jenkins' method[1] is similar to Worthing's method since it also involves

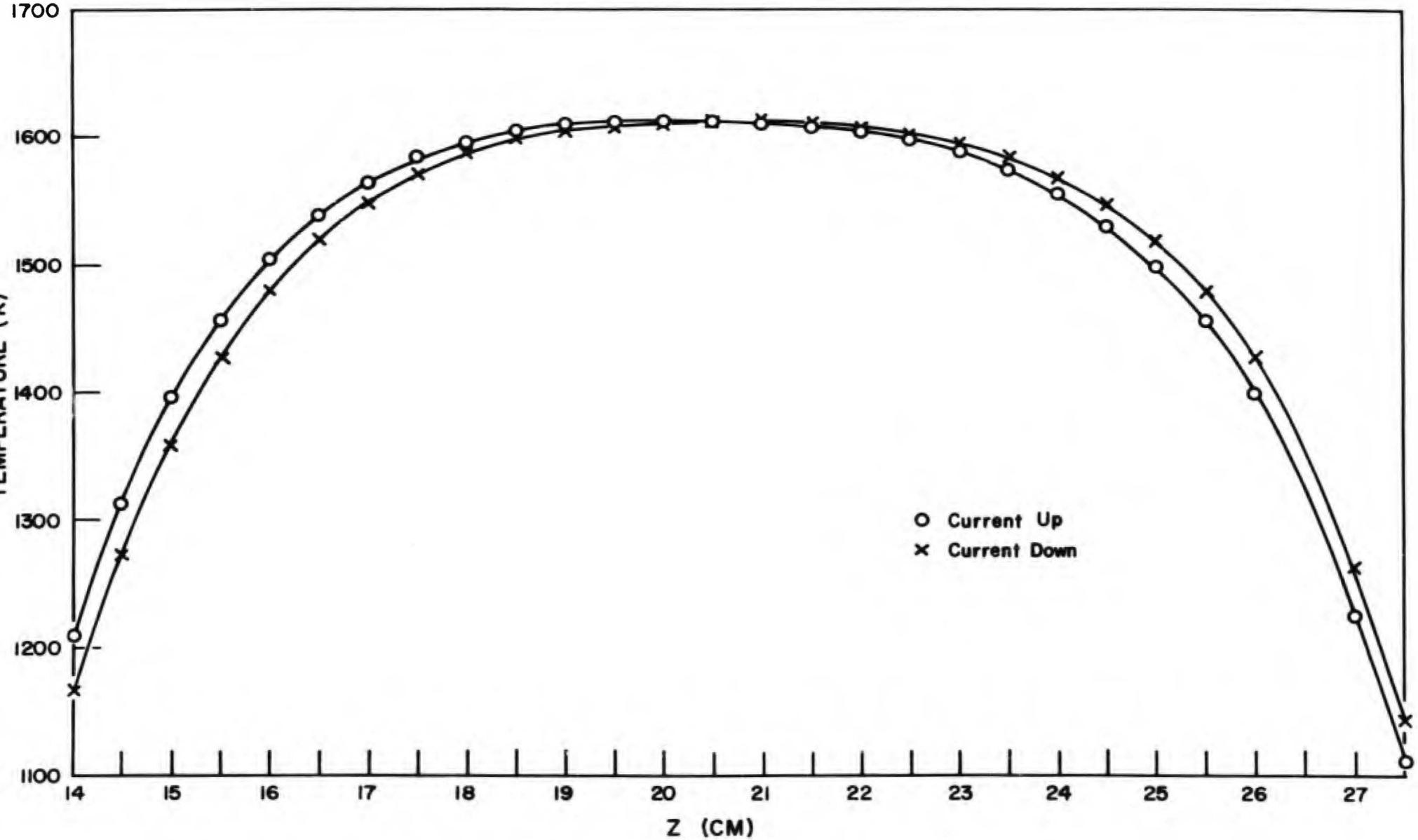

FIGURE 18 TEMPERATURE PROFILES FOR TANTALUM
(90 AMPS, 7" SAMPLE)

Note: Reverse page 58 is blank.

graphical integration. However, Worthing's integration is over a geometrical interval instead of a temperature interval. Worthing's results for tantalum are shown in Figure 17. The uncertainties in both the Worthing and Rudkin et al. methods appear to be relatively large (primarily because of a $(dT/dZ)^{-2}$ or corresponding term), and both methods are inconvenient due to the graphical integrations. Consequently, results using the present data were not calculated for these methods. Bode's method was not investigated because it is applicable only to small diameter samples of materials with an appreciable temperature coefficient of resistivity.

B. ATJS Graphite

Samples of Grade ATJS Graphite were obtained from the Air Force Materials Laboratory of Wright-Patterson Air Force Base. Grade ATJS Graphite is an improved version of ATJ graphite produced by Union Carbide Corporation. Like ATJ graphite, it is molded graphite having a maximum particle size of 0.006", but differs in that it is impregnated after the carbonization cycle, with the material being carbonized again and then graphitized. Thus, Grade ATJS Graphite has a higher density (nominally 1.8 gm cm^{-3}) than ATJ (about 1.7 gm cm^{-3}) and is more uniform. The densities of the samples tested were 1.806 to 1.809 gm cm^{-3} when measured by water immersion, and 1.902 to 1.910 gm cm^{-3} when measured by alcohol immersion. Only samples machined perpendicular ($\perp$) to the molding direction were received and investigated. The spectral emittance at 0.65 microns was determined by measuring the brightness temperature of the surface of electrically-heated thin-walled tubes and the temperature of the cavity. Two sizes of tubes were used; 5/8" OD by 1/2"ID and 3/8" OD by 1/4"ID. Calculations indicated that the temperature drop across the walls of these cylinders should be less than 2 degrees below 2500 K. The spectral emittance results for the two samples are shown in Figure 19. These results are believed to be accurate within 1%, and the two curves are separated by an amount equal to their combined uncertainty. It should be noted that changing the spectral emittance by 1% at 1600 K corresponds to changing the "true temperature" of the graphite surface by 1.4 K. Because the values of ϵ_λ for graphite were not measured on the identical samples used for the resistivity, total hemispherical emittance and thermal conductivity measurements, the uncertainty as to which ϵ_λ values to use causes uncertainties in the value of these properties. Consequently, ρ, ϵ_{II} and λ values were calculated using both ϵ_λ curves shown in Figure 19. The resulting ϵ_{II} values differed by almost 1% but both ρ and λ values were changed by less than 0.2%. Thus, the uncertainty in ϵ_λ of graphite did not seriously affect the thermal conductivity results.

Electrical resistivity and total hemispherical emittance were measured simultaneously on two 1/8" diameter rods used for the conductivity determinations. The electrical resistivity results (⊥) are shown in Figure 20. The electrical resistivity (in ohm cm) from 1200 to 2400 K of the first sample can be expressed as:

$$\rho = 5.2195 \times 10^{-4} + 1.3296 \times 10^{-7}T + 6.6049 \times 10^{-12}T^2. \qquad (\perp)$$

The resistivity (in ohm cm) of the second sample from 1300 to 2600 K is about 1% less and is given by

$$\rho = 4.7419 \times 10^{-4} + 1.8055 \times 10^{-7}T - 6.8767 \times 10^{-12}T^2. \qquad (\perp)$$

Additional resistivity measurements were obtained on a 1/4" diameter rod. These results were very close to the lower curve shown in Figure 20. These measurements further demonstrated that the electrical resistivity exhibits a minimum below 1100 K and that the values then increase to about 860×10^{-6} ohm cm near room temperature.

The total hemispherical emittance results for the two samples are given in Figure 21. The data for the first sample were obtained during seven separate runs (including runs both before and after temperature profile measurements) and above 1200 K can be expressed as

$$\epsilon_H = 0.7533 + 8.278 \times 10^{-6}T$$

As shown in Figure 21, the values for the total hemispherical emittance of the second sample were within 1% of those measured for the first sample.

Thermal conductivity values for the two graphite samples are given in Figure 22. Conductivity data on the first sample were obtained from 10 different profiles. About 500 conductivity values were calculated from these profiles using the 3-point method. Since this is too many values to plot conveniently, only results of the "multiple-point" methods (Figure 16) are given on Figure 22. Although fewer profiles were obtained on the second sample, the results definitely tended to be lower than those obtained for the first sample (Figure 22). Smoothed conductivity values for the two samples are given in Table 7.

The recommended curve[7] for Grade ATJ Graphite is included on Figure 22. From this figure, it is deduced that the conductivity of Grade ATJS Graphite is about

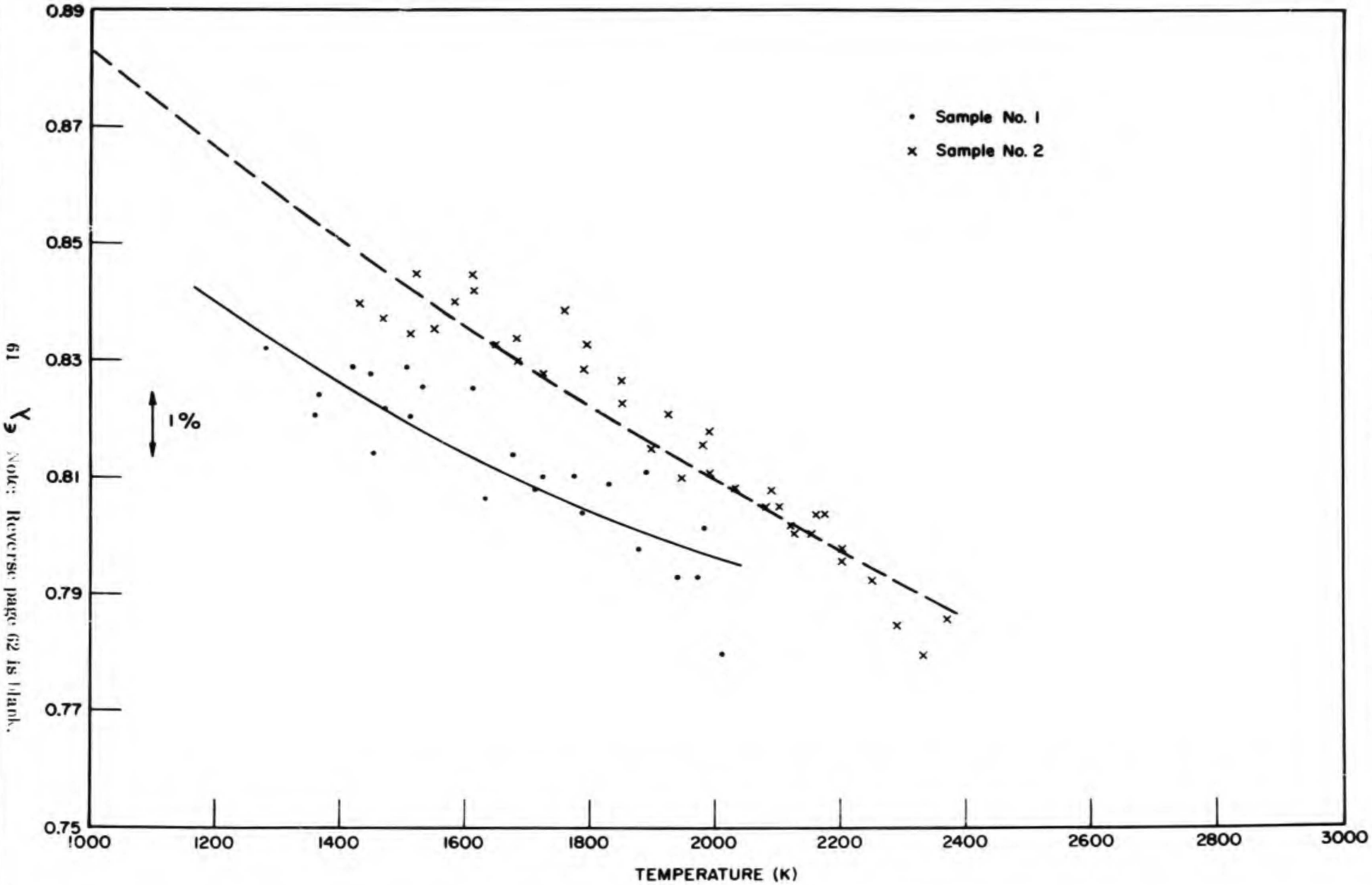

FIGURE 19 SPECTRAL EMITTANCE (0.65 MICRONS) OF GRADE ATJS GRAPHITE

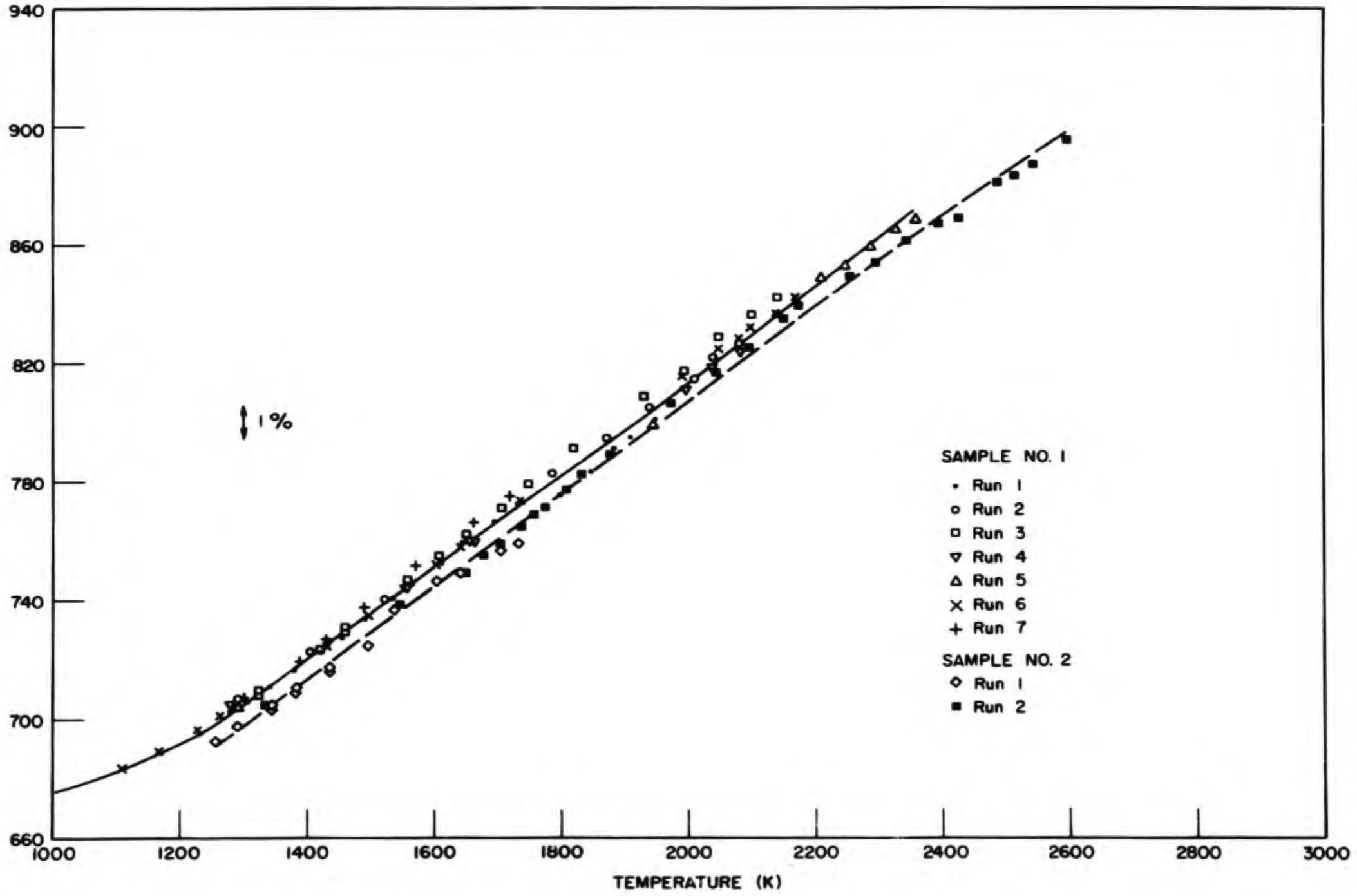

63

Note: Reverse page 64 is blank.

FIGURE 20 ELECTRICAL RESISTIVITY OF GRADE ATJS GRAPHITE (⊥)

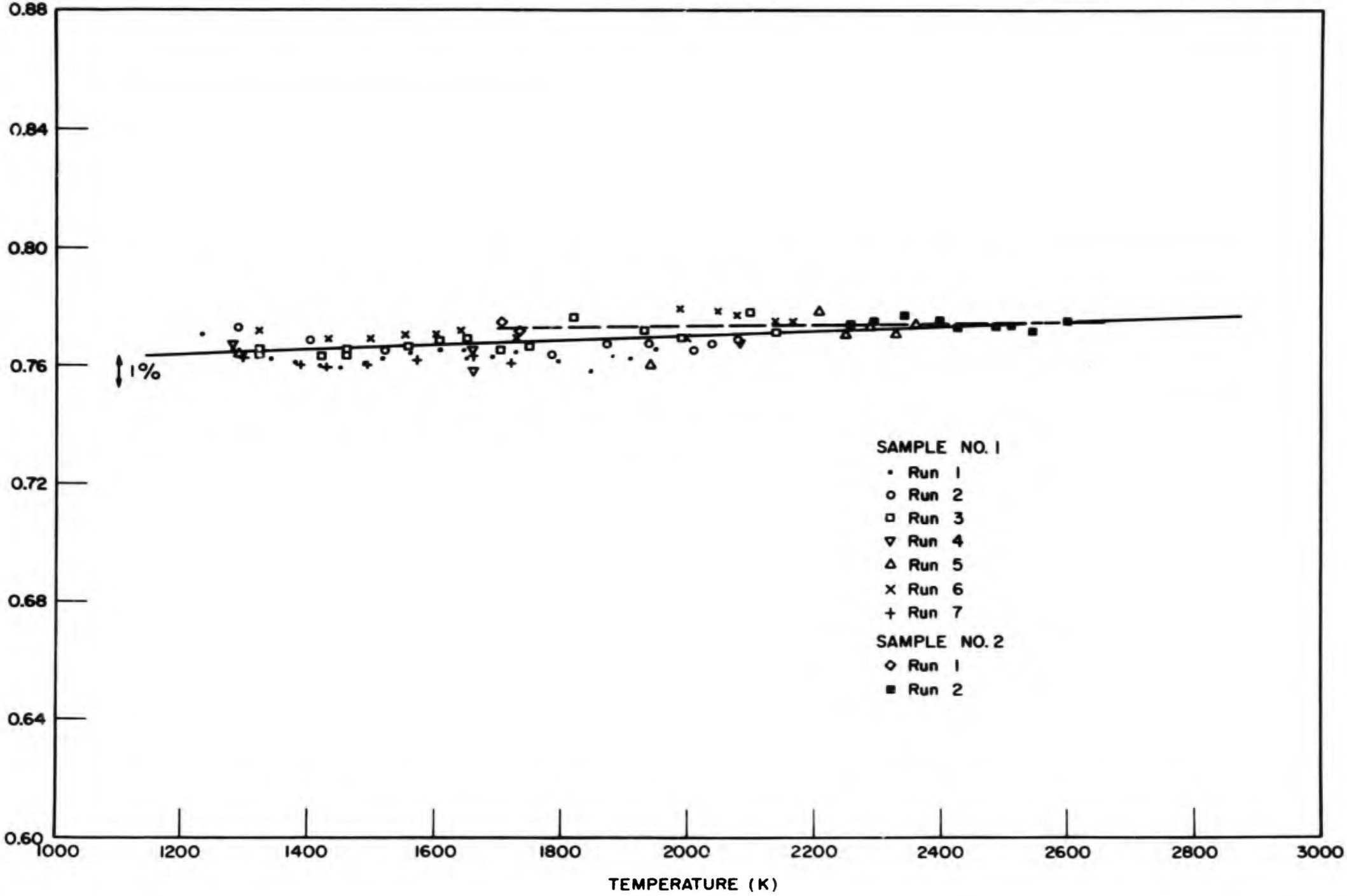

FIGURE 21 TOTAL HEMISPHERICAL EMITTANCE OF GRADE ATJS GRAPHITE

Note: Reverse page 66 is blank.

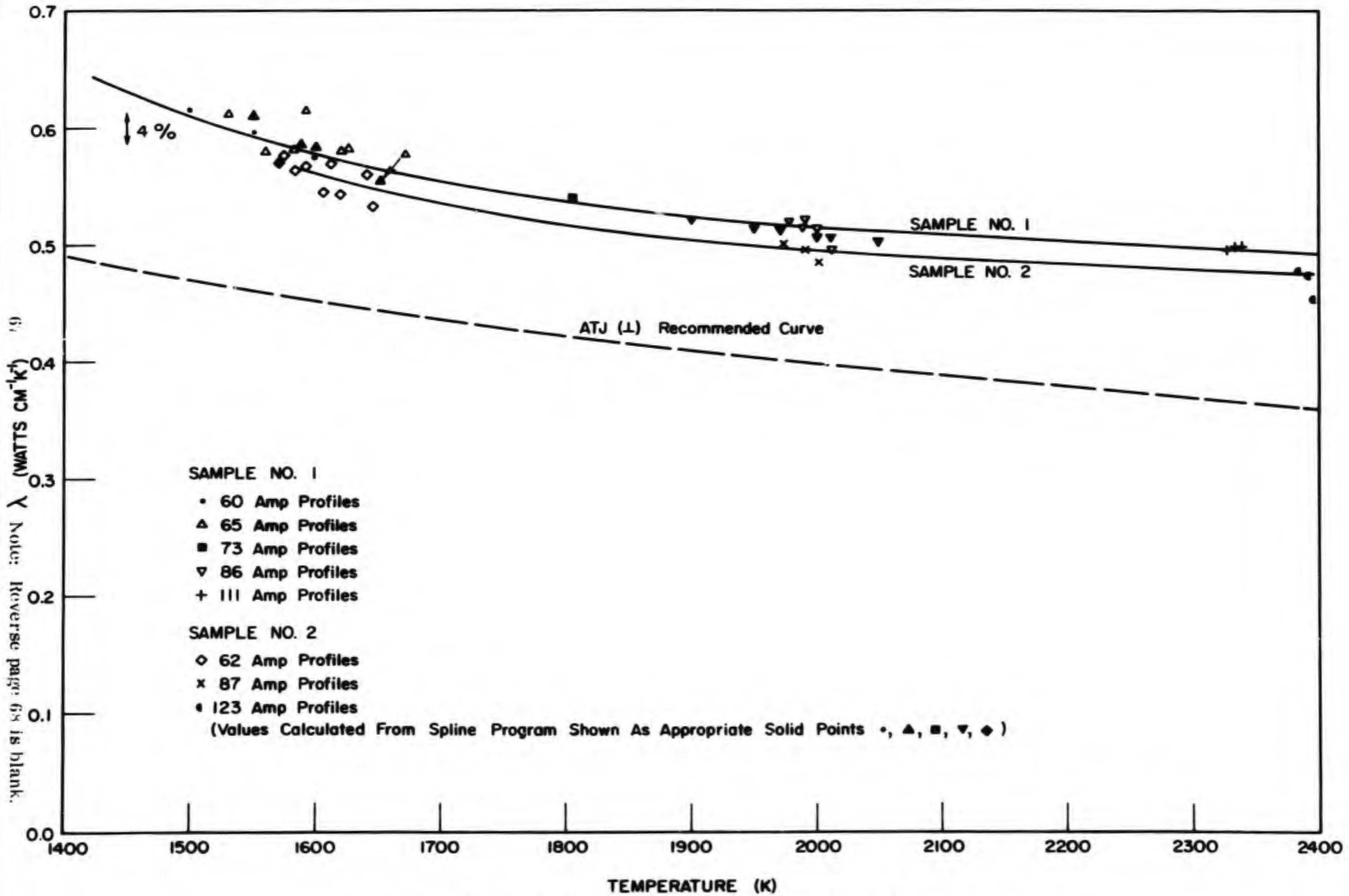

FIGURE 22 THERMAL CONDUCTIVITY OF GRADE ATJS GRAPHITE (⊥)

Note: Reverse page 69 is blank.

20% greater than that of ATJ Graphite. This observation indicates that the difference in conductivity values between the two grades of graphite is much greater than the difference in densities (about 5%).

Conductivity values were also calculated from several of the profiles using the Krishnan and Jain and the Lebedev techniques. These results were disappointing in that they were usually more than 10% above the values given in Figure 22 or Table VIII.

TABLE VIII

THERMAL CONDUCTIVITY AND LORENZ FUNCTION OF GRADE ATJS GRAPHITE(⊥)

Temp. (K)	Thermal Conductivity (W $cm^{-1}K^{-1}$)		Lorenz Function (10^{-8} W ohms K^{-2})
	Sample 1	Sample 2	Sample 1
1500	0.610	-	29.9
1600	0.578	0.561	27.2
1700	0.554	0.535	25.0
1800	0.541	0.515	23.5
1900	0.524	0.504	22.0
2000	0.515	0.495	21.0
2100	0.509	0.490	20.1
2200	0.503	0.484	19.4
2300	0.497	0.479	18.6
2400	0.492	0.475	18.0

Also included in Table VIII are values of the Lorenz function calculated using the resistivity and the conductivity values for sample number 1. The values of the Lorenz function are much greater than the theoretical value for metals of 2.443×10^{-8} W ohm K^{-2} and are also greater than some other values published for graphite[24]. These results demonstrate that the lattice component of the conduction mechanism is still important in graphite at high temperatures and/or that the electronic component is considerably different from that observed in metals.

C. Tungsten

Several samples of tungsten (originally manufactured by Climax Molybdenum Corporation) were purchased from A.D. Little, Inc. These samples are from the same batch used in the Air Force sponsored high temperature thermal conductivity standards program.[25] The densities of the two samples used in the property deter-

minations were found to be 19.23 gm cm^{-3} by the water immersion technique. The material was arc cast, extruded, stress relieved and recrystallized at 1925 K prior to delivery. The nominal composition was reported[25] to be 99.87% W minimum, 0.1% Mo maximum and to include various gaseous and metallic impurities in the ppm range.

Prior to measurements, Sample 1 and Sample 2 were aged in vacuum at 2750 and 2980 K respectively for several hours. This aging caused significant grain growth and embrittlement. During the final resistivity measurements following the temperature profile measurements, the first sample was jarred and separated along grain boundaries into three pieces. Similarly, the second sample parted along grain boundaries into two samples during a spot-welding operation in conjunction with the final resistivity measurements.

During a test, the second sample was subjected to a temperature of 3087 K, which was higher than its aging temperature of 2980 K. A noticeable vaporization occurred. fogging the quartz viewing window. As a result of this heating, the sample geometry changed slightly and the total hemispherical emittance changed several percent. A new emittance curve was generated and additional profiles were measured. The latter data is referred to as Sample 2, Part 2 (W-2-2) in this report, while the data obtained on the sample prior to the vaporization is denoted as Sample 2, Part 1 (W-2-1).

The electrical resistivity data for the three samples (W-1, W-2-1, and W-2-2) are shown on Figure 23. The results in ohm cm can be expressed as:

$$\rho = -3.4286 \times 10^{-6} + 2.65671 \times 10^{-8}T + 1.7770 \times 10^{-12}T^2 \quad (1600 < T < 2650\ K)\ W\text{-}1$$

$$\rho = -4.0937 \times 10^{-6} + 2.73239 \times 10^{-8}T + 1.5454 \times 10^{-12}T^2 \quad (1600 < T < 2810\ K)\ W\text{-}2\text{-}1$$

$$\rho = -3.0617 \times 10^{-6} + 2.63091 \times 10^{-8}T + 1.7265 \times 10^{-12}T^2 \quad (1650 < T < 2690\ K)\ W\text{-}2\text{-}2$$

These values are in excellent agreement with data reported by Osborn[27] and Platunov and Fedoror[28] and are in fair agreement with the data of Pears[26] and Rudkin, Barker, and Jenkins[29]. However, the values of Tye[9] and Forsythe and Worthing[30] are as much as 5% greater than the present results at the higher temperatures.

The total hemispherical emittance data for the three tungsten samples are shown in Figure 24. The data can be expressed as:

$$\epsilon_H = 1.35 \times 10^{-2} + 1.36146 \times 10^{-4}T - 1.1784 \times 10^{-8}T^2 \quad (1600<T<2650\ K)\ W\text{-}1$$

$$\epsilon_H = -2.99 \times 10^{-2} + 1.8799 \times 10^{-4}T - 2.3485 \times 10^{-8}T^2 \quad (1600<T<2810\ K)\ W\text{-}2\text{-}1$$

$$\epsilon_H = 16.40 \times 10^{-2} + 1.5340 \times 10^{-4}T - 1.6543 \times 10^{-8}T^2 \quad (1650<T<2690\ K)\ W\text{-}2\text{-}2$$

These results are in good agreement with the data of Abbott[16] and Allen, Glasier and Jordan[21], since their data indicate that the emittance increases from about 0.20 at 1700 K to 0.30 at 2800 K.

The spectral emittance data (0.65 microns) of the three samples are given in Figure 25. It is noted that there is a correlation between the total and spectral emittances of the samples, i.e. the sample with the highest total hemispherical emittance has the highest spectral emittance. Previously reported spectral emittance values (0.65 microns) for tungsten are 0.42 by Larrabee[31] and 0.37 by Allen, Glasier and Jordan[21] (both observed over wide temperature ranges). The present results for samples W-1 and W-2-2 are between these values while the results for W-2-1 are somewhat greater than Larrabee's values.

The thermal conductivity results for tungsten are shown in Figure 26. These results are primarily those obtained by averaging the computer outputs for the current up and down profiles using the spline program for fitting $T(Z)$, dT/dZ and d^2T/dZ^2 (Figure 16). Some points were calculated using d^2T/dZ^2 derived from the 3-point method (Figure 16). Although data from the samples overlap, the results are best represented by two curves, one for the first sample (W-1) and one for the second sample (W-2-1 and W-2-2). These least-squares curves may be represented by:

$$\lambda = -1.5419 \times 10^{-4}T + 1.3073 \quad (1850<T<2400\ K)\ (W\text{-}1)$$

$$\lambda = -1.1041 \times 10^{-4}T + 1.193 \quad (1700<T<2800\ K)\ (W\text{-}2\text{-}1 \text{ and } W\text{-}2\text{-}2)$$

Actually, the difference between the two curves is within the experimental accuracy and one is justified in combining all the data into one least squares fit given by:

$$\lambda = -1.1890 \times 10^{-4}T + 1.219 \quad (1700<T<2800\ K)\ (\text{combined data})$$

In Figure 27 the present thermal conductivity results are compared with literature values obtained using direct electrical heating methods[1] and with the TPRC recommended curve[32]. The results of Allen, Glasier and Jordan[21], Worthing[19] and Zwikker[33] are about 50% above the present results at the higher temperatures, while the values of Rudkin, Parker and Jenkins[29] are about 20% below the present results. Thus, the conductivity values previously obtained for tungsten by direct electrical heating methods are widely scattered. However, the results of Gumenyuk, Ivanov and Lebedev[22] and Gumenyuk and Lebedev[34], also obtained by direct heating methods are only about 5% from the recommended curve, which is partly based on the data for all methods. The present results lie between those of Gumenyuk, Ivanov and Lebedev[22] and Gumenyuk and Lebedev[34] and those of the recommended curve[32].

The thermal conductivity of tungsten samples from the same batch as that used in the present work were measured by several laboratories as part of a round-robin program[25]. Two laboratories (General Electric and Illinois Institute of Technology) measured the thermal conductivity while two other laboratories (Atomics International and Battelle Memorial Institute) computed the conductivity for the results of thermal diffusivity measurements. Since the latter two sets of results (AI and BMI) depend upon the values of specific heat used in the calculations, only the GE and IIT results are compared with the present measured values in Figure 28. The present values lie between the GE and IIT results. It should be noted[25] that the BMI high temperature data tends to support the IIT results while the AI data tends to support the GE results.

Additional measurements on similar samples of tungsten are planned by a number of laboratories[25]. In order to facilitate future comparisons, the present experimental data points are given in Table IX.

Using the combined curves for λ and ρ, values of the Lorenz function given in Table X were computed. These values are appreciably above the theoretical value for "good" metals, even at very high temperatures. However, they are in reasonable agreement with the results of Gumenyuk and Lebedev[34] which indicate that the Lorenz function decreases from 2.91×10^{-8} at 1173 K to 2.73×10^{-8} at 1573 K and is almost independent of temperature above 1573 K. Recent observations for other transition metals have also indicated that the Lorenz function is greater than the theoretical value at high temperatures.[35]

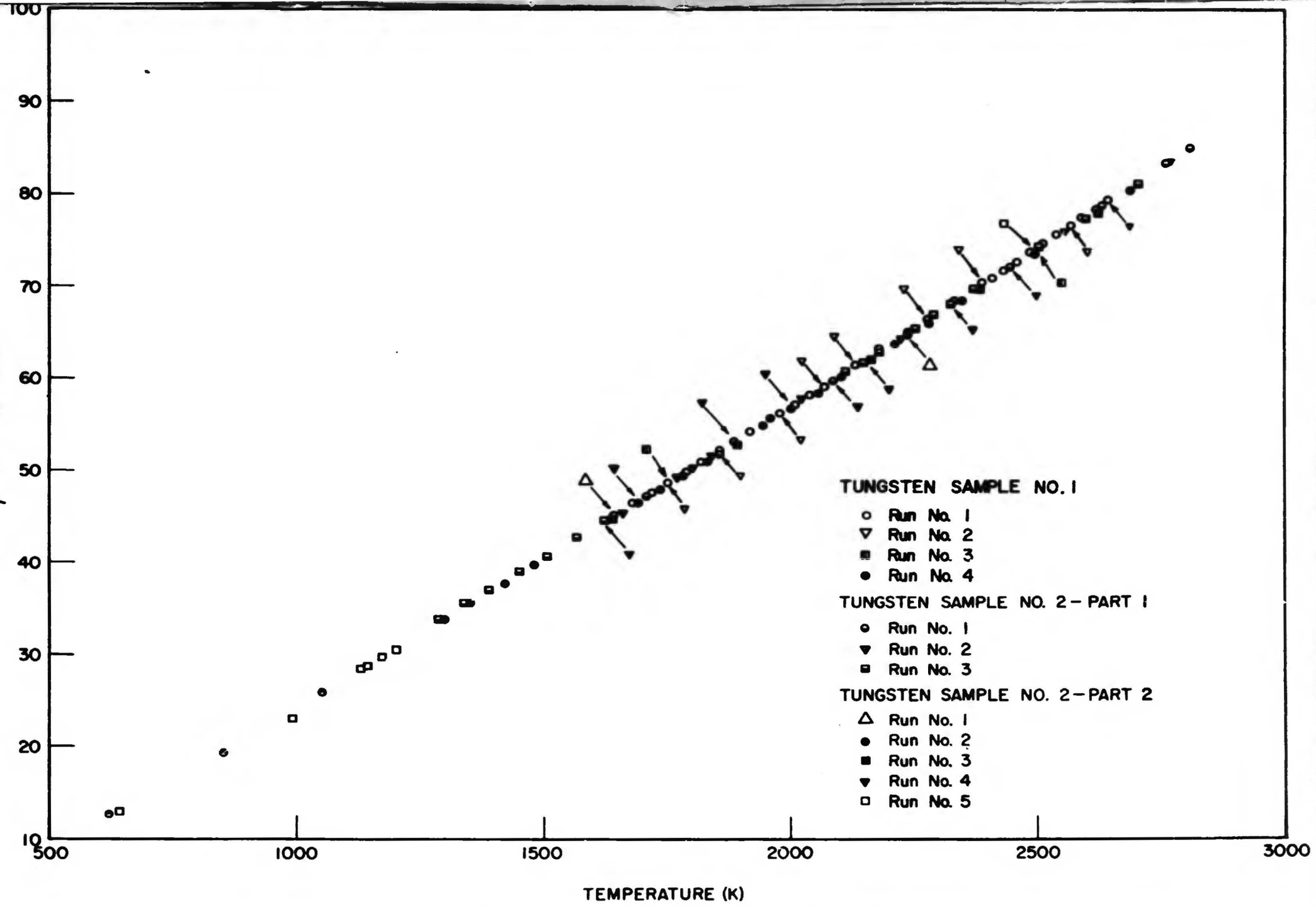

FIGURE 23 ELECTRICAL RESISTIVITY OF TUNGSTEN

 Note: Reverse page 74 is blank.

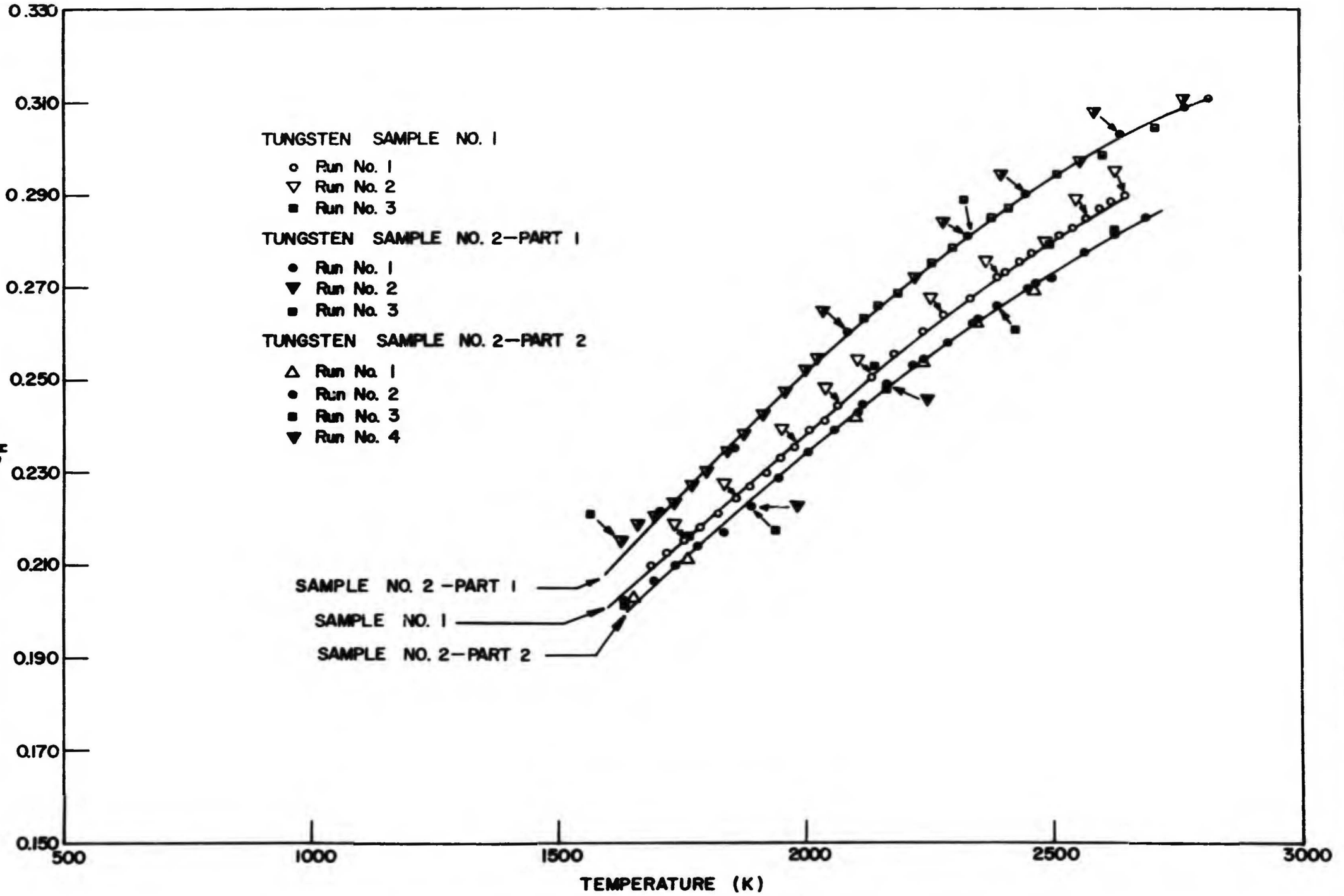

FIGURE 24 TOTAL HEMISPHERICAL EMITTANCE OF TUNGSTEN

75 Note: Reverse page 76 is blank.

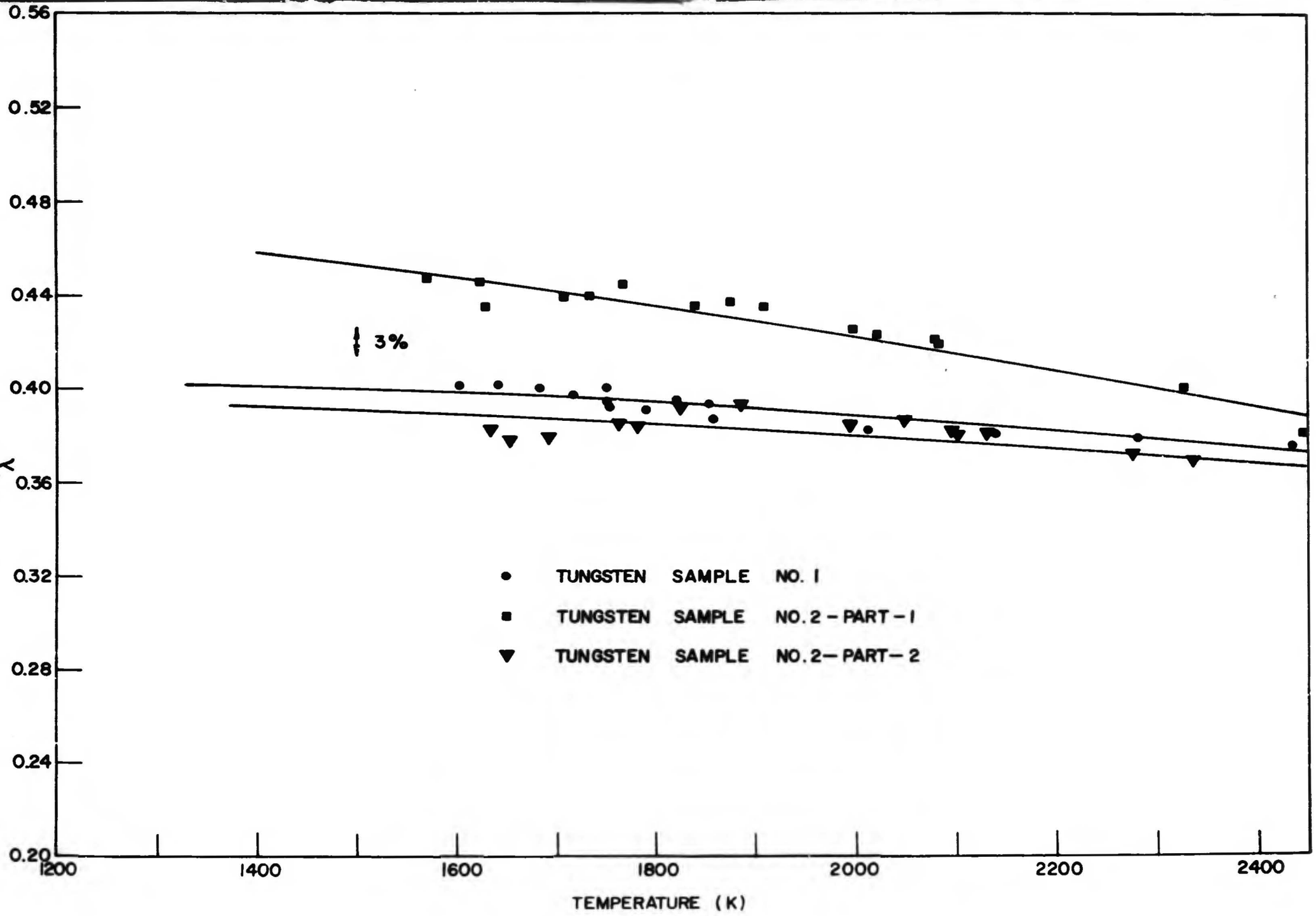

FIGURE 25 SPECTRAL EMITTANCE (0.65 MICRONS) OF TUNGSTEN

Note: Reverse page 75 is blank.

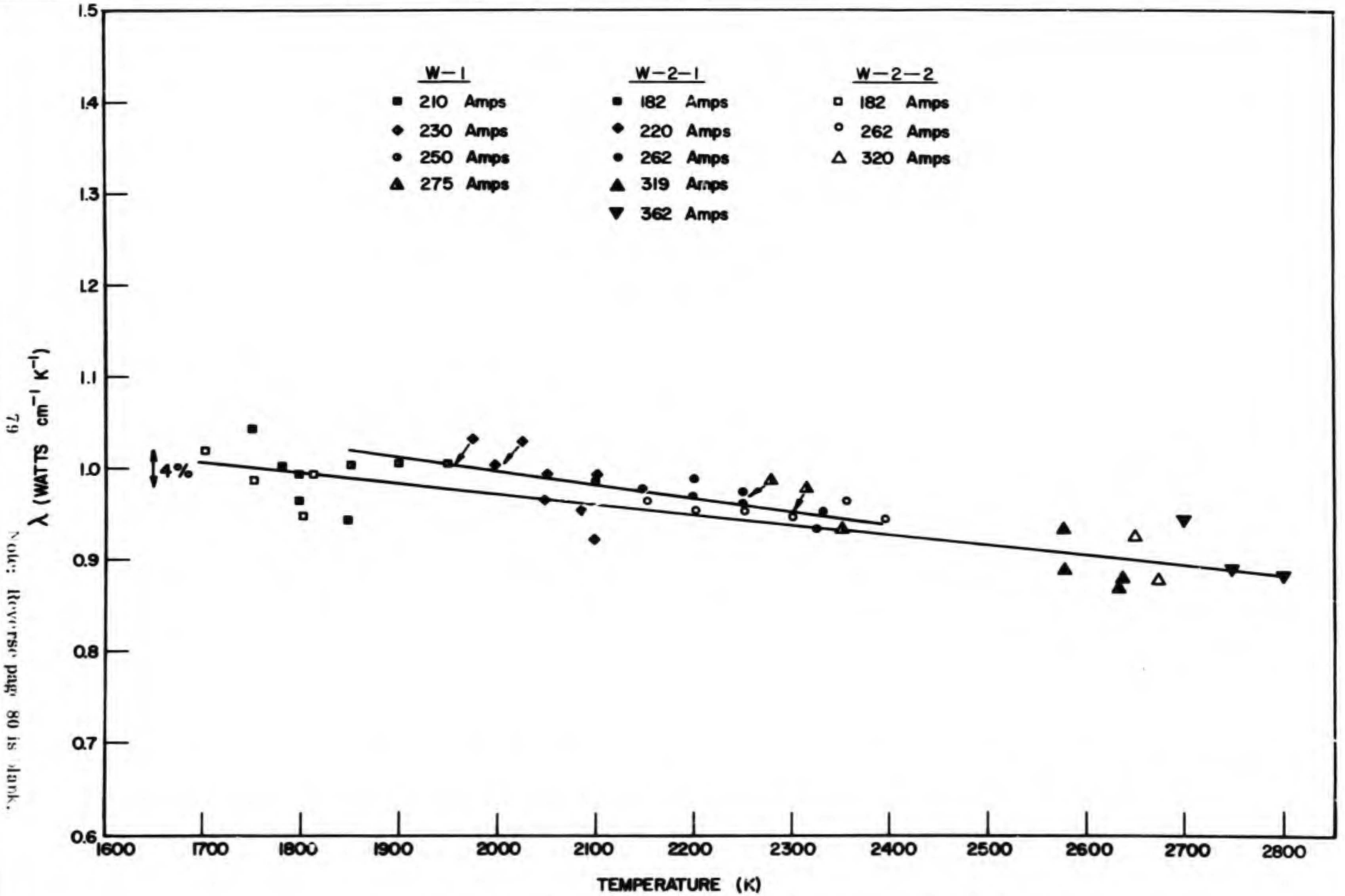

FIGURE 26 THERMAL CONDUCTIVITY OF TUNGSTEN (EXPERIMENTAL DATA)

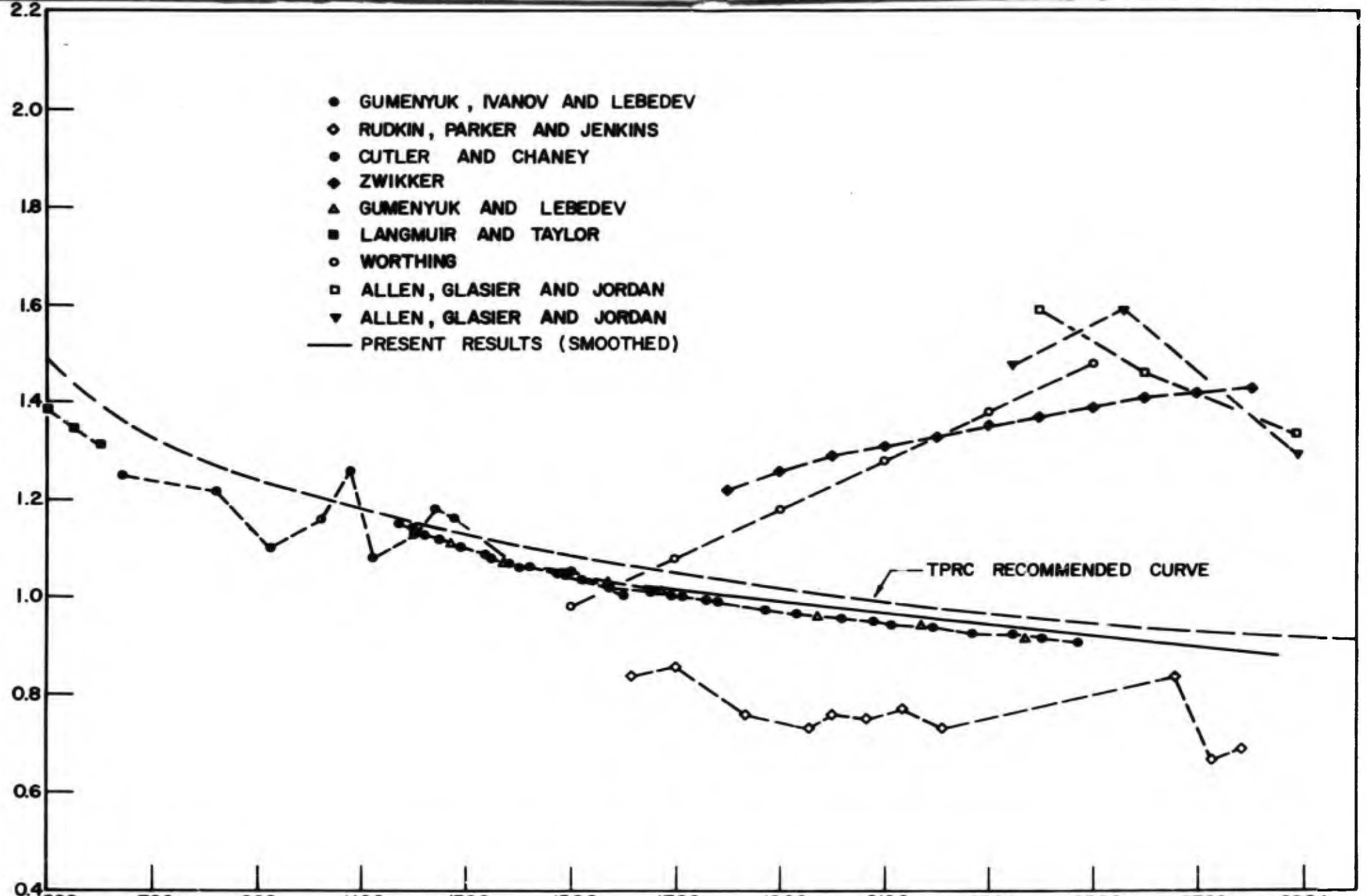

FIGURE 27 THERMAL CONDUCTIVITY OF TUNGSTEN (ELECTRICAL METHODS)

Note: Reverse page 2 is blank.

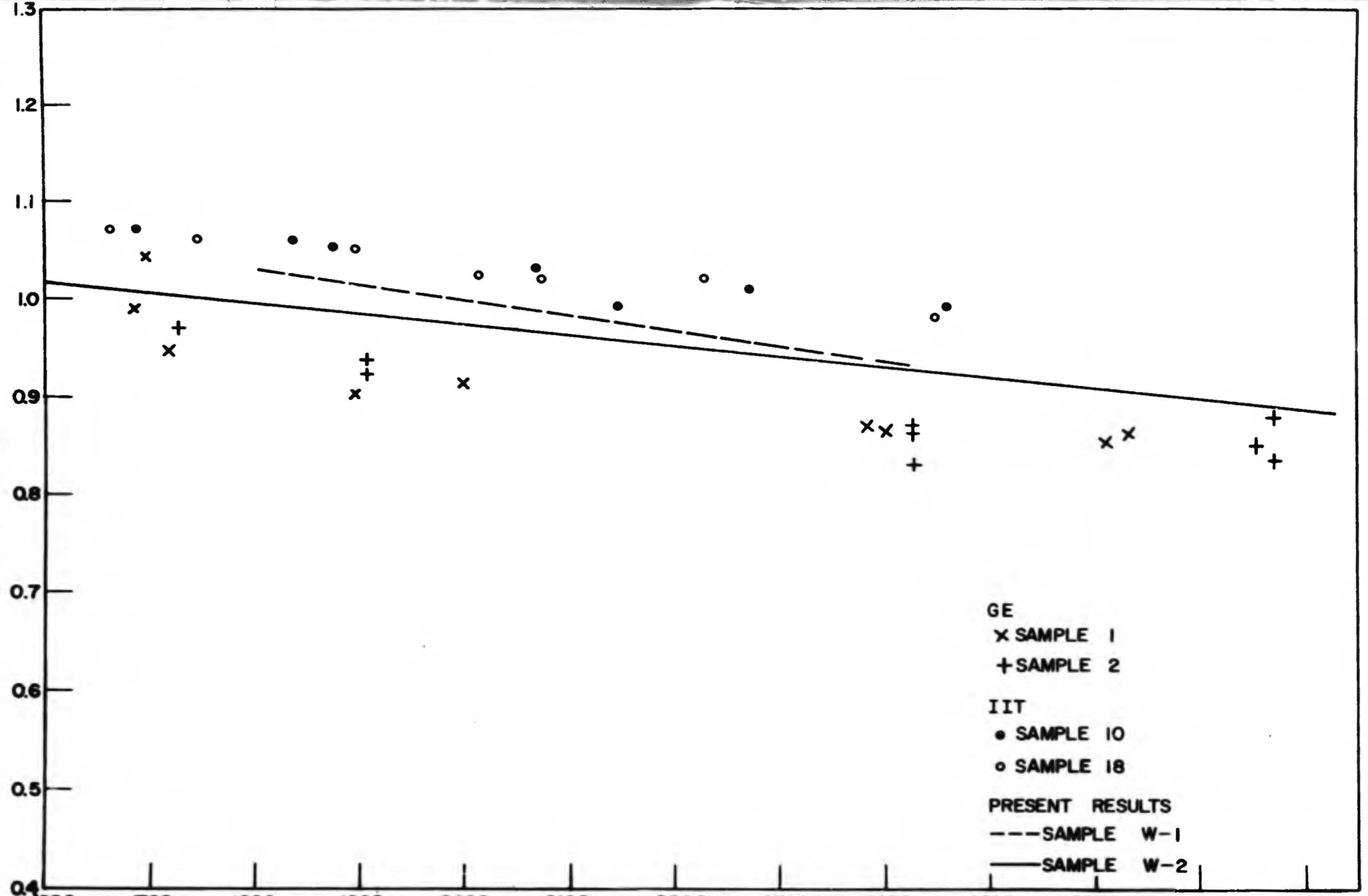

FIGURE 28 THERMAL CONDUCTIVITY OF TUNGSTEN (ROUND ROBIN RESULTS)

Note: Reverse page 84 is blank.

BLANK PAGE

TABLE IX

EXPERIMENTAL THERMAL CONDUCTIVITY VALUES FOR TUNGSTEN

First Tungsten Sample (W-1)

210 amp profile		230 amp profile		250 amp profile		275 amp profile	
T(K)	λ (W $cm^{-1}K^{-1}$)	T(K)	λ (W $cm^{-1}K^{-1}$)	T(K)	λ (W $cm^{-1}K^{-1}$)	T(K)	λ (W $cm^{-1}K^{-1}$)
1850.0	1.004	1950.0	1.010	2100.0	0.987	2250.0	0.964
1900.0	1.005	2000.0	1.005	2150.0	0.979	2300.0	0.948
1950.0	1.006	2050.0	1.000	2200.0	0.972	2350.0	0.932
		2100.0	0.994	2250.0	0.964	2400.0	0.916

Second Tungsten Sample (W-2) - Parts 1 and 2

182 amp - Part 1		220 amp - Part 1		262 amp - Part 1		319 amp - Part 1	
T(K)	λ (W $cm^{-1}K^{-1}$)	T(K)	λ (W $cm^{-1}K^{-1}$)	T(K)	λ (W $cm^{-1}K^{-1}$)	T(K)	λ (W $cm^{-1}K^{-1}$)
1750.0	1.042	2000.0	1.013	2200.0	0.992	2577.0	0.939
1800.0	0.994	2050.0	0.967	2250.0	0.977	2579.0	0.888
1850.0	0.941	2100.0	0.920	2327.8	0.929	2632.3	0.870
1796.0	0.960	2085.0	0.953	2322.4	0.957	2640.9	0.879
1780.0	1.007						
362 amp - Part 1		182 amp - Part 2		262 amp - Part 2		320 amp - Part 2	
T(K)	λ (W $cm^{-1}K^{-1}$)	T(K)	λ (W $cm^{-1}K^{-1}$)	T(K)	λ (W $cm^{-1}K^{-1}$)	T(K)	λ (W $cm^{-1}K^{-1}$)
2700.0	0.904	1700.0	1.023	2150.0	0.964	2676.0	0.875
2750.0	0.889	1750.0	0.986	2200.0	0.959		
2800.0	0.873	1800.0	0.949	2250.0	0.954		
		1825.0	0.993	2300.0	0.949		
				2356.0	0.968		
				2392.0	0.947		

TABLE X

THERMAL CONDUCTIVITY AND LORENZ FUNCTION FOR TUNGSTEN
(SAMPLE 2)

T(K)	λ (W $cm^{-1}K^{-1}$)	ρ (10^{-6} ohm cm)	L(10^{-8} W ohm K^{-2})
1700	1.005	46.653	2.758
1800	0.994	49.888	2.755
1900	0.983	53.158	2.750
2000	0.972	56.462	2.744
2100	0.961	59.801	2.737
2200	0.950	63.174	2.728
2300	0.939	66.582	2.718
2400	0.928	70.025	2.708
2500	0.917	73.501	2.696
2600	0.906	77.013	2.684
2700	0.895	80.559	2.670
2800	0.884	84.139	2.656

IV. STATUS OF PROGRAM

The experimental apparatus is operational to temperatures of about 2800 K at 2×10^{-7} torr. Electrical resistivity, total hemispherical emittance and spectral emittance data are routinely obtained up to this temperature. Temperature profiles, from which thermal conductivity values can be computed using the mathematical schemes outlined in this report, are also routinely obtained.

Measurements on a number of materials of interest to the Air Force Materials Laboratory have been made, and others, including ZrB_2, are contemplated. The extension of the capabilities of the system to include measurements on fiber and fine wires is under investigation.

Improvements in data analysis procedures, to fully utilize the advantages of the multiple point technique, is underway. In particular, automatic schemes to incorporate the 3-point dT/dZ values are being investigated as well as schemes which separate the data profiles into symmetrical and nonsymmetrical parts. The latter procedure could appreciably improve Thomson coefficient results. The improvements will lead to optimized measurement techniques. At present, temperature profile data are obtained at equal space intervals. The results to date indicate that a different measurement scheme would appreciably improve the conductivity results. The feasibility of digitalized data recording will be incorporated as part of the improved measurement techniques.

In addition, it has become very obvious that the basic method is capable of yielding accurate data simultaneously and/or concurrently on a number of additional thermophysical properties for the same sample in the same apparatus. These properties include specific heat, enthalpy, Richardson coefficient, Seebeck coefficient, Peltier coefficient, coefficient of linear expansion and thermal diffusivity. It is hoped that funding to permit the increasing modifications to permit the incorporation of these measurements will become available.

V. SUMMARY AND CONCLUSIONS

The temperature range of the multiple purpose apparatus was extended from 1800 to about 2800 K by the incorporation of a high current (500 amps) regulated DC power supply. Other recent modifications included additional protection against oil backstreaming into the high vacuum enclosure and the installation of a movable tantalum tube heater for high temperature resistivity measurements. Novel developments are "clamp-on" blackbody cavities and voltage probes.

Substantial improvements in the numerical methods of "solving" the second order non-linear differential equation governing thermal transport in thin current-carrying samples having been made. These techniques include the 3-point method which permits computation of a conductivity value using any three temperature position data points from a temperature profile. Under development are techniques which utilize data from the entire profile. Conductivity values obtained by these multiple point techniques are more accurate and exhibit much less scatter than values obtained by the 2- or 3-point methods. Some of these techniques yield values of the Thomson coefficient in addition to the conductivity value.

The results of measurements on tantalum, ATJS graphite and tungsten are reported. These include total hemispherical emittance, spectral emittance, electrical resistivity and thermal conductivity. Reproducibilities of the emittance and resistivity were usually within ±1% up to 2800 K. Thermal conductivity values computed using multiple point techniques were generally within ±3% of a smooth line representing conductivity versus temperature. The accuracies are primarily limited by the accuracy of the temperature measurements and are believed to be less than ±1% for the resistivity, ±2% for the emittance and ±5% for the conductivity.

The present results and those given in a previous report[2] have shown that several of the previously published direct heating methods are capable of yielding conductivity values accurate within 10% under optimum conditions, but that the range of acceptable conditions is quite limited when compared to the general methods developed during the present project.

VI. REFERENCES

(1) Powell, R.W., DeWitt, D.P. and Nalbantyan, M., "The Precise Determination of Thermal Conductivity and Electrical Resistivity of Solids at High Temperatures by Direct Electrical Heating Methods", AFML-TR-67-241, 1967.

(2) Taylor, R.E., Powell, R.W., Nalbantyan, M. and Davis, F., "Evaluation of Direct Electrical Heating Methods for the Determination of Thermal Conductivity at Elevated Temperatures", AFML-TR-68-227, 1968.

(3) Quinn, T.J. and Barber, C.R., "A Lamp as a Reproducible Source of Near Blackbody Radiation for Precise Pyrometry up to 2700 C", Metrologia, 3(1), 19-23, 1967.

(4) Lee, R.D., "Construction and Operation of a Simple High-Precision Copper-Point Blackbody and Furnace", NBS Technical Note 483, May 1969.

(5) Flynn, D.R., "Measurement of Thermal Conductivity by Steady-State Methods in Which the Sample is Heated Directly by Passage of an Electric Current", Thermal Conductivity, Vol. 1, Chap. 5, edited by R.P. Tye, Academic Press, N.Y., 1969.

(6) Rice, J.R., "Approximation Formulas for Physical Data", Pyrodynamics 6, 231-256, 1968.

(7) Ho, C.Y., Powell, R.W. and Liley, P.E., "Thermal Conductivity of Selected Materials, Part 2", NSRDS-NBS 16, U.S. Government Printing Office, February 1968.

(8) Taylor, R.E. and Finch, R.A., "The Specific Heats and Resistivities of Molybdenum, Tantalum and Rhenium", J. Less-Common Metals, 6, (4), 283-294, 1964.

(9) Tye, R.P., "Preliminary Measurements of the Thermal and Electrical Conductivities of Molybdenum, Niobium, Tantalum and Tungsten", J. Less-Common Metals, 3, 13-18, 1961.

(10) Gumenyuk, V.S., Ivanov, V.E. and Lebedev, V.V., "Determination of the Heat and Electric Conductivity of Metals at Temperatures in Excess of 1000 C", Instrum. Exper. Techn. (U.S.A.) No. 1, 188-92, 1962.

(11) Petrov, V.A., Chekhovskoi, V.Ya. and Sheindlin, A.E., "Integral Hemispherical Radiating Power and Specific Electrical Resistance of Tantalum in the Temperature Interval 1200-2800 K", High Temperature, 6(3), 525-6, May - June 1968.

(12) Touloukian, Y.S., Ed., "Thermophysical Properties of High Temperature Solid Materials", Vol. I, Elements, 944, Macmillan Co., N.Y., 1967.

(13) Butler, C.P., Jenkins, R.J., Rudkin, R.L. and Laughridge, F.I., "High Temperature Surface Parameters for Solar Power" from Coatings for the Aerospace Environment, 229-252, USNRDL, San Francisco, Calif., 1961.

(14) Malter, L. and Langmuir, D.B., "Resistance, Emissivities and Melting Point of Tantalum", Phys. Rev. 55, 743-7, 1939

(15) Schwartz, H., Ed., "Determination of the Emissivity of Materials" Annual Progress Rept. from Pratt and Whitney Aircraft, East Hartford, Conn., Jan. 1-Dec. 31, 1963. PWA-2309, NASA-CR-58054 N 64-26808.

(16) Abbott, G.L., "Total Normal and Total Hemispherical Emittance of Polished Metals - Part III", U.S. Naval Radiological Defense Lab., 30 pp., 1963.

(17) Peletskii, V.E. and Voskresenskii, V.Yu., "Thermophysical Properties of Tantalum at Temperatures Above 1000 C", High Temperature, 4(3), 329-33, 1966.

(18) Serebryakova, T.I., Paderno, Yu.B. and Samsonov, G.V., "Emission Coefficients of Some Powdered High-Melting Compounds", Optics and Spectroscopy, 8, 212 213, 1960.

(19) Worthing, A.G., "The Thermal Conductivities of Tungsten, Tantalum and Carbon at Incandescent Temperatures by an Optical Pyrometer Method", Phys. Rev. 4(6), 535-43, 1914.

(20) Rasor, N.S. and McClelland, J.D., "Thermal Properties of Graphite, Molybdenum and Tantalum to Their Destruction Temperatures", Intl. Jour. Phys. Chem. Solids, 15, 17-26, 1960.

(21) Allen, R.D., Glasier, L.F., Jr. and Jordan, P.L., "Spectral Emissivity, Total Emissivity and Thermal Conductivity of Molybdenum, Tantalum and Tungsten Above 2300 K", J. Appl. Phys. 31(8), 1382-7, 1960.

(22) Gumenyuk, V.S., Ivanov, V.E. and Lebedev, V.V., "Determination of the Thermal Conductivity of Metals at Temperatures Above 1000 K", Teplo i Massoperenos, Pervoe Vses. Soveshch, Minsk, 1, 94-101, 1962.

(23) Jun, C.K. and Hoch, M., "Thermal Conductivity of Tantalum, Tungsten, Rhenium, Ta-10W, T_{111}, T_{222}, W-25Re in the Temperature Range 1500-2800 K", AFML-TR-66-367, 17 pp., 1966.

(24) Powell, R.W. and Schofield, F.H., "The Thermal and Electrical Conductivities of Carbon and Graphite to High Temperatures", Proc. Phys. Soc. 51 (1), 153-172, 1939.

(25) A.D. Little, Inc., "Development of High Temperature Thermal Conductivity Standards", AFML-TR-69-2, June 1969.

(26) Pears, C.D., "The Thermal Properties of Twenty-Six Solid Materials to 5000 F or Their Destruction Temperatures", Southern Research Inst., Birmingham, Ala., 420 pp., 1962, ASD-TDR-62-765. [AD 298061]

(27) Osborn, R.H., "Thermal Conductivities of Tungsten and Molybdenum at Incandescent Temperatures", J. Optical Soc. Am. 31, 428-32, 1941.

(28) Platunov, E.S. and Fedorov, V.B., "Use of Photographic Pyrometry in Thermal Studies", High Temperature 2(4), 568-72, 1964. English Translation from Teplofizika Vysokikh Temperatur 2(4), 628-33, 1964.

(29) Rudkin, R.L., Parker, W.J. and Jenkins, R.J., "Measurements of the Thermal Properties of Metals at Elevated Temperatures", Temperature - Its Measurement and Control in Science and Industry, Vol. 3, Pt. 2, Reinhold Publishing Corp., N.Y., 523-34, 1962.

(30) Forsythe, W.E. and Worthing, A.G., "The Properties of Tungsten and the Characteristics of Tungsten Lamps", Astrophys. J. 61, 146-185, 1925.

(31) Larrabee, R.D., "Spectral Emissivity of Tungsten", J. Opt. Soc. Am. 49(6), 619-25, 1959.

(32) Powell, R.W., Ho, C.Y. and Liley, P.E., "Thermal Conductivity of Selected Materials", NSRDS-NBS 8, U.S. Government Printing Office, November, 1966.

(33) Zwikker, C., "Physical Properties of Tungsten at High Temperature", Archives Neerlandaises des Sciences Exactes et Naturelles, III A (9), 207-339, 1925.

(34) Gumenyuk, V.S. and Lebedev, V.V., "Investigation of the Thermal and Electrical Conductivity of Tungsten and Graphite at High Temperatures", Phys. Metals and Metallog. U.S.S.R. 11(1), 30-5, 1961.

(35) Williams, R.K. and Fulkerson, W., "Separation of the Electronic and Lattice Contributions to the Thermal Conductivity of Metals and Alloys", Thermal Conductivity Proceedings of the Eighth Conference, edited by C.Y. Ho and R.E. Taylor, Plenum Press, N.Y., 389-456, 1969.

(36) Cutler, M. and Cheney, G.T., "Measurement of Thermal Conductivity of Electrical Conductors at High Temperatures", J. Appl. Phys., 34(6), 1714-8, 1963.

(37) Langmuir, I. and Taylor, J.B., "The Heat Conductivity of Tungsten and the Cooling Effects of Leads on Filaments at Low Temperatures", Phys. Rev., 50(1), 68-87, 1936.

Security Classification

DOCUMENT CONTROL DATA - R & D

(Security classification of title, body of abstract and indexing annotation must be entered when the overall report is classified)

1. ORIGINATING ACTIVITY *(Corporate author)*

Thermophysical Properties Research Center

2a. REPORT SECURITY CLASSIFICATION

Unclassified

2b. GROUP

3. REPORT TITLE

Determination of Thermal and Electrical Conductivity, Emittance and Thomson Coefficient at High Temperatures by Direct Heating Methods

4. DESCRIPTIVE NOTES *(Type of report and inclusive dates)*

Annual Progress Report August 1, 1968 to July 31, 1969

5. AUTHOR(S) *(First name, middle initial, last name)*

Raymond E. Taylor, Frederick E. Davis, Reginald W. Powell and Wilbur D. Kimbrough

6. REPORT DATE	7a. TOTAL NO. OF PAGES	7b. NO. OF REFS
October 1969	90	37

8a. CONTRACT OR GRANT NO.

F33(615)-69-C-1229

b. PROJECT NO.

7381

c.

Task No. 738106

d.

9a. ORIGINATOR'S REPORT NUMBER(S)

9b. OTHER REPORT NO(S) *(Any other numbers that may be assigned this report)*

AFML-TR-69-277

10. DISTRIBUTION STATEMENT

This document has been approved for public release and sale; its distribution is unlimited.

11. SUPPLEMENTARY NOTES

12. SPONSORING MILITARY ACTIVITY

Air Force Materials Laboratory, Wright-Patterson Air Force Base

13. ABSTRACT

Progress on a program for evaluating direct electrical heating methods for high temperature thermal conductivity determinations is presented. Recent modifications, which increased the temperature capabilities of the apparatus, protected the samples from contamination and improved the accuracy and simplicity of the measurements, are described.

A method for calculating the thermal conductivity using any three temperature versus position data points (3-point method) of a temperature profile was devised. Using this 3-point method, hundreds of conductivity values can be calculated per temperature profile. Computational schemes which utilize multiple data points or the output of the 3-point program are being developed. Substantial improvement in the accuracy and reproducibility of the computed thermal conductivity values has been obtained using these schemes. In addition, values for the Thomson coefficient are derived.

Data on thermal conductivity, total hemispherical emittance, spectral emittance (0.65 microns), electrical resistivity, and Thomson coefficients for tantalum, ATJS graphite and tungsten to about 2700 K are presented. Reproducibilities were generally about ±0.7% for the electrical resistivity, ±1% for the total hemispherical emittance, ±1% for the spectral emittance and ±3% for the thermal conductivity (multiple data point computations).

DD FORM 1 NOV 65 1473

Security Classification

14. KEY WORDS	LINK A		LINK B		LINK C	
	ROLE	WT	ROLE	WT	ROLE	WT
Thermal Conductivity						
Electrical Resistivity						
Total Hemispherical Emittance						
Spectral Emittance						
Thomson Coefficient						
ATJS Graphite						
Tantalum						
Tungsten						
Lorenz Function						